Supporting Information (SI)

Dissecting Multivalent Lectin-Carbohydrate Recognition Using Polyvalent Multifunctional Glycan-Quantum Dots

Yuan Guo[1,*], Inga Nehlmeier[2], Emma Poole[1], Chadamas Sakonsinsiri[1,6] Nicole Hondow[3], Andy Brown[3], Qing Li[4], Shuang Li[5], Jessie Whitworth[1], Zhongjun Li[4], Anchi Yu[5], Rik Brydson[3], W. Bruce Turnbull[1], Stefan Pöhlmann[2], and Dejian Zhou[1,*]

[1] School of Chemistry and Astbury Centre for Structural Molecular Biology, University of Leeds, Leeds LS2 9JT, United Kingdom.

[2] Infection Biology Unit, German Primate Center, Kellnerweg 4, 37077 Gottingen, Germany.

[3] School of Chemical and Process Engineering, University of Leeds, Leeds LS2 9JT, UK.

[4] Department of Chemical Biology, Peking University Health Sciences Centre, Beijing 100191, P.R. China.

[5] Department of Chemistry, Renmin University of China, Beijing 100872, P.R. China.

[6] Current Address: Department of Biochemistry, Faculty of Medicine, Khon Kaen University, Khon Kaen 40002, Thailand.

Contents

1: Material, instrument and methods

1.1) Materials

CdSe/ZnS core/shell QDs (λ_{EM} ~560 nm) was purchased commercially from PlasmaChem GmbH (Berlin, Germany). The QDs were supplied as dry powders capped with mixed ligands of trioctylphosphine oxide (TOPO), hexadecylamine and oleic acid. A CdSe/ZnSe/ZnS core/shell/shell QD capped with mixed ligands of TOPO and trioctylphospine (λ_{EM} ~605 nm) in toluene was purchased from STREM chemicals UK Ltd. O-(2-Aminoethyl)-O′-(2-azidoethyl)decylethylene glycol (N_3-EG_{11}-NH_2, >95% oligomer purity) was purchased from Polypure Plc (Norway). Azido-3,6,9-trioxaundecan-1-amine (N_3-EG_3-NH_2, >90% monomer purity), N,N-dimethyl-1,3-propanediamine (>99%), 1,3-propane-sultone (> 99%), lipoic acid (LA, >99%), triphenyl-phosphine (>98.5%), dicyclohexylcarbodiimide (DCC, >99%), dimethylaminopyridine (DMAP, >99%), tris(2-carboxyethyl)phosphine hydrochloride (TCEP.HCl, >98%), triethylamine (>99%), chloroform (> 99.8%), magnesium sulphate (>99%), methanol (> 99.9%), potassium hydroxide, ethylacetate (>99.0%), methylene chloride (>98%), sodium bicarbonate (>99.5%) and other chemicals were purchased from Sigma-Aldrich (Dorset, UK) and used as received without further purification unless stated otherwise. Solvents were obtained from Fisher Scientific (Loughborough, UK) and used as received. Ultra-pure water (resistance >18.2 MΩ.cm) purified by an ELGA Purelab classic UVF system, was used for all experiments and making buffers.

1.2) Instrument and Methods

All moisture-sensitive reactions were performed under a N_2 atmosphere using oven-dried glassware. Dry solvents were obtained through an innovative technology solvent drying system. Evaporations were performed under reduced pressure on a rotary evaporator. The synthesis was monitored by TLC on silica gel 60 F254 plates on aluminum and stained by iodine. Flash column chromatography was performed on silica gel 60 A (Merck grade 9385). All ^1H and ^{13}C NMR spectra are recorded on Brucker DPX300 (500 MHz for ^1H, 125 MHz for ^{13}C) in $CDCl_3$ except for azide-modified mannoses which were recorded on a 300 MHz machine (75 MHz for ^{13}C NMR). All chemical shifts were reported in parts per million (ppm). The coupling constants were given in Hz. Assignment of ^1H NMR spectra was achieved using 2D methods (COSY) when necessary. The abbreviations used in ^1H NMR analysis are: s = singlet, br = broad, d = doublet, t = triplet, q = quartet, m = multiplet, dd = double doublet.

High resolution mass spectra (HR-MS) were obtained on a Bruker Daltonics MicroTOF mass spectrometer. Infra-red spectra were recorded on a PerkinElmer FT-IR spectrometer. Melting points were obtained on a Griffin melting point apparatus. Optical rotations were measured at the sodium D-line with a Schmidt + Haensch Polartronic H532 polarimeter. $[\alpha]_D$ values were given in units of 10^{-1} deg cm^2 g^{-1}. UV-vis absorption spectra were recorded on a Varian Cary 50 bio UV-Visible Spectrophotometer over 200-800 nm using 1 mL quartz cuvette with an optical path of 1 cm or on a Nanodrop 2000 spectrophotometer (Thermo scientific) over the range of 200-800 nm using 1 drop of the solution with an optical path length of 1 mm. All centrifugations were carried out on a Thermo Scientific Heraeus Fresco 21 microcentrifuge using 1.5 mL microcentrifuge tubes at room temperature (unless stated otherwise). The QD purification was performed in Amicon ultra-

centrifugal filter tubes with a cut-off MW of 30,000. Dynamic light scattering (DLS) was measured on a Zetasizer Nano (Malvern) using a final C_{QD} of 40 nM. The hydrodynamic sizes (D_hs) of the QD-EG_n-DiMan only were measured in pure water and binding buffer (50 mM HEPES, 100 mM NaCl, 10 mM $CaCl_2$, pH 7.8). The D_hs of the QD/protein assembly were measured in binding buffer containing 40 nM QD and 500 nM protein (all final concentration) as described previously.

All fluorescence spectra were measured on a Cary Eclipse Fluorescence Spectrophotometer using a 0.70 mL quartz cuvette. All measurements were done in a binding buffer (20 mM HEPES, 100 mM NaCl, 10 mM $CaCl_2$ pH 7.8) containing 0.1 mg/mL of a His_6-Cys peptide which we have previously found to increase the stability of the QD in buffer.[1,2] The QDs were mixed with the calculated amount of labeled proteins thoroughly in the binding buffer at room temperature (RT) for 20 min before fluorescence spectra were recorded. An excitation wavelength (λ_{EX}) of 450 nm, corresponding to the λ_{Abs} minimum of the Atto594 dye (acceptor), was used in all the fluorescence measurement to minimise the direct excitation background. The fluorescence emission spectra over 500-750 nm was recorded at a scan rate of 120 nm/min. For wild-type protein competition assay, unlabeled wild-type protein stocks were prepared first in the binding buffer. Then different amount of the wild-type protein was mixed with the labeled DC-SIGN (final labeled $C_{DC\text{-}SIGN}$ = 0.5 μM) first before being added to the QD-EG_n-DiMan (final C_{QD} = 40 nM, labeled DC-SIGN:QD molar ratio =12.5) in building buffer. The resulting solutions were further incubated at RT for 20 min before fluorescence spectra were recorded.

The fluorescence lifetimes of the QD and dye FRET signals were recorded using a home-built time correlated single photon counting apparatus.[3] The output (460 nm) of an optical parametric amplifier pumped by a Spectra Physics 1 kHz amplified Ti:sapphire laser system was used as the excitation source. A singlet lens was used to focus the excitation beam into the sample (QD-EG_{11}-DiMan only, QD-EG_{11}-DiMan + DC-SIGN (Atto-594 labeled) at a QD:protein molar ratio of 3, 10 or 30 respectively) and the subsequent fluorescence was collected in a back scattering geometry with a parabolic mirror. The emission was sent into a Princeton Instruments SP2358 monochromator where the signal from the QD (λ_{EM} ~560 nm) and the dye FRET (λ_{EM} ~630 nm) were separated and detected with a Hamamatsu R3809U-50 MCP-PMT. The signal was amplified by a Becher & Hickl GmbH HFAC-26 preamplifier. The output of the HFAC-26 preamplifier and the output of a fast PicoQuant TDA 200 photodiode were connected to a Becher & Hickl GmbH SPC-130 module as the start and stop pulses respectively. Magic angle detection was used to avoid the effect of molecular reorientation. The full-width at half-maximum (FWHM) of the instrumental response function (IRF) of this setup was determined to be ~70 ps.[3]

2. Synthesis of the DHLA-EG_n-glycan ligands[1,2,4,5]

The synthetic route to the DHLA-EG_n-glycan ligands (where n = 3 or 11 stands for uniform length oligo-(ethylene glycol) containing 3 or 11 ethylene glycol units) is shown in Scheme 1. The synthesis of the mannose terminating ligands (DHLA-EG_n-Man, where n = 3 or 11) has been reported previously.[1]

2.1) Step i: Synthesis of lipoic acid-oligo(ethylene glycol)-azide (LA-EG_n –N_3)

LA-EG$_{11}$-N$_3$,[2,5] N$_3$-EG$_{11}$-NH$_2$ (0.481g, 0.843 mmol), DCC (0.222 g, 1.011 mmol) and lipoic acid (LA, 0.1733 g, 0.843 mmol) was dissolved in DCM (10 mL) and stirred under a N_2 atmosphere and cooled to 0˚C by an ice bath. To this solution, DMAP (0.022 g, 0.1686 mmol) in DCM (5 mL) was added slowly over a period of 5 to 10 minutes. The mixture was then stirred for 1 hour under an ice bath and then left to warm up RT and stirred for a further 8 hours. The crude product was then filtered up and the solid residue was washed with a small amount of DCM. The combined filtrate and DCM washing solution were combined and evaporated to dryness on a rotary evaporator. The residue was purified by column chromatography on a silica gel column using a mixed solvent of MeOH and $CHCl_3$ (1:10, vol/vol). The eluted solution was checked by TLC and the fractions containing pure LA-EG$_{11}$-N$_3$ was combined and evaporated to dryness, yielding the desired compound as a yellow oil (0.417 g, 0.549 mmol, 65 % yield). **TLC:** (MeOH/$CHCl_3$ 1:10) R_f = 0.42. **^{1}H-NMR** (400 MHz, $CDCl_3$): δ 6.16 (s, br, 1H), 3.76-3.53 (m, 22H), 3.49 (t, J= 5 Hz, 2H), 3.38 (t, J = 5 Hz, 2H), 3.32 (t, J = 5.2 Hz, 2H), 3.15 (m, 2H), 2.39 (m, 1H), 2.12 (t, J = 7.7 Hz, 2H), 1.84 (m, 1H), 1.60 (m, 4H), 1.51 (s, 1H), 1.40 (m, 2H). **^{13}C-NMR** (125 MHz, $CDCl_3$): δ 172.8 (C, C_{25}), 70.7 – 70.0 (20C, C_3-C_{23}), 56.5 (C, C_{30}), 50.7 (C, C_{24}), 40.2 (C, C_{31}), 39.2 (C, C_1), 38.5 (C, C_{32}), 36.3 (C, C_{29}), 34.7 (C, C_{26}), 28.9 (C, C_{28}), 25.4 (C, C_{27}). **FT-IR**: 3321.94; 2915.70; 2859.78; 2099.40; 1649.64; 1539.87; 1448.58; 1078.13 cm^{-1}. **MS**: calcd *m/z* for $C_{32}H_{62}N_4O_{12}S_2Na$ $(M + Na)^+$ = 781, found 781.00.

LA-EG$_3$-N$_3$, N$_3$-EG$_3$-NH$_2$ (1.0 g, 4.58 mmol), DCC (1.040 g, 5.04 mmol) and DMAP (0.0895 g, 0.733 mmol) was prepared in dry DCM (20 mL). The mixture was cooled to 0˚C in an ice bath under a N_2 atmosphere. TA (0.95 g, 4.58 mmol) dissolved in 4 mL dry DCM was slowly added through a syringe over 20 minutes again under a nitrogen atmosphere. After addition, the reaction was left stirring at 0˚C for 1 hour before being left to gradually warm up to RT and stirred for a further 24 hours. The reaction mixture was filtered and the insoluble solid was washed with $CHCl_3$. The filtrate and wash solutions were combined and evaporated to dryness to yield the crude product. The product was then purified by silica gel column chromatography (MeOH:CH_2Cl_2, v/v = 1:16) and checked by TLC. The fractions containing pure LA-EG$_3$-N$_3$ were combined and evaporated to dryness, yielding the desired compound as a yellow oil in 94% yield (1.7489 g, 4.302 mmol). **TLC:** (MeOH/CH_2Cl_2 1:16) R_f = 0.60. **^{1}H-NMR** (400 MHz, $CDCl_3$): δ 6.002(s, br, 1H), 3.67 (m, 14H), 3.47 (t, 2H), 3.41 (t, 2H), 3.19 (t, 2H), 3.14 (m, 2H), 2.37 (m, 1H), 2.21 (t, 2H), 1.93 (m, 1H), 1.71 (m, 4H), 1.48 (s, 1H). **^{13}C-NMR** (100 MHz, $CDCl_3$): δ 172.7 (C, C_9), 70.8 – 69.9 (5C, C_2-C_7), 56.4 (C, C_{14}), 50.7 (C, C_8), 40.3 (C, C_{15}), 39.2 (C, C_1), 38.5 (C, C_{16}), 36.4 (C, C_{13}), 34.7 (C, C_{10}), 28.9 (C, C_{12}), 25.4 (C, C_{11}). **IR**: 3322.13; 2925.81; 2854.16; 2099.05; 1647.28; 1536.02; 1438.58; 1105.23 cm^{-1}. **MS**: calculated *m/z* for $C_{16}H_{31}N_4O_4S_2$ $(M+ H)^+$ = 407, found 407.8.

2.2) Step ii: Synthesis of LA-EG$_n$-NH$_2$

LA-EG$_{11}$-NH$_2$: LA-EG$_{11}$-N$_3$ (0.417 g, 0.549 mmol) and PPh_3 (0.321 g, 1.098 mmol) were dissolved in dry THF (10 mL) and stirred under a nitrogen atmosphere at RT for 30 minutes. H_2O (0.11 mL) was then added and the reaction solution was stirred at RT for a further 48 hours till all the LA-EG$_{11}$-N$_3$ was reduced completely. TLC was used to check for the reaction (MeOH: $CHCl_3$, 1:4 (vol/vol)) against the starting materials to confirm the azide reduction. The resulting product was then purified by silica gel column chromatography

using MeOH: $CHCl_3$, 1:4 (vol/vol) as eluting solvent. The fractions containing the desired compound were combined and evaporated to dryness, yielding LA-EG_{11}-NH_2 as a yellow oil (0.1448 g, 0.1975 mmol, 35 % yield). **TLC:** (MeOH/$CHCl_3$ 1:4) R_f = 0.31. **^{1}H-NMR** (400 MHz, $CDCl_3$): δ 6.37 (s, br, 1H), 3.69 – 3.53 (m, 44H), 3.48 (m, 2H), 3.17 (m, 2H), 2.90 (m, 2H), 2.81 (s, br, 2H), 2.48 (m, 1H), 2.21 (m, 2H), 1.93 (m, 1H), 1.70 (m, 4H), 1.41 (m, 2H). **^{13}C-NMR** (125 MHz, $CDCl_3$): δ 172.9 (C, C_{25}), 70.6 – 70.2 (20C, C_3-C_{23}), 56.5 (C, C_{30}), 41.7 (C, C_{24}), 40.2 (C, C_{31}), 39.2 (C, C_1), 38.5 (C, C_{32}), 36.3 (C, C_{29}), 34.7 (C, C_{26}), 28.9 (C, C_{28}), 25.4 (C, C_{27}). **MS**: calcd *m/z* for $C_{32}H_{65}N_2O_{12}S_2$ $[M + H]^+$ = 733, found 734.00.

LA-EG_3-NH_2: TA-EG_3-N_3 (1.7489 g, 4.302 mmol) and triphenylphosphine (2.257 g, 8.604 mmol) were dissolved in dry THF (30 mL) and then stirred for 1 hour at RT under N_2. Next degassed H_2O (1.55 mL, 86.04 mmol) was added to the reaction mixture and left to stir for a further 20 hours. The solvent was removed and crude product was purified using silica gel chromatography. Firstly the by-products were eluted using MeOH: $CHCl_3$ 1:9 and then the desired product was eluted using MeOH: $CHCl_3$ 3:7. The fractions containing the desired compound were combined and evaporated to dryness, yielding LA-EG_3-NH_2 as a yellow oil (1.4117 g, 3.710 mmol, 86 % yield). **TLC:** (MeOH/$CHCl_3$ 3:7) R_f = 0.1. **^{1}H-NMR** (400 MHz, $CDCl_3$): δ 6.61 (s, br, 1H), 3.36-3.59 (m, 14H), 3.11 (m, 1H), 3.08 (m, 1H), 2.79 (m, 2H), 2.73 (br, 2H), 2.45 (m, 1H), 2.23 (m, 2H), 1.89 (m, 2H), 1.40-1.66 (m, 8H). **^{13}C-NMR** (100 MHz, $CDCl_3$): δ 172.9 (C, C_9), 70.6 – 70.1 (5C, C_2-C_7), 56.5 (C, C_{14}), 50.8 (C, C_8), 40.3 (C, C_{15}), 39.2 (C, C_1), 38.5 (C, C_{16}), 36.3 (C, C_{13}), 34.7 (C, C_{10}), 29.0 (C, C_{12}), 25.4 (C, C_{11}). **IR**: 3344.51; 2926.03; 2862.35; 1672.85; 1599.66; 1271.59; 1006.00 cm^{-1}. **MS**: calcd *m/z* for $C_{16}H_{33}N_2O_4S_2$ $[M+ H]^+$ = 381.2, found 381.4.

2.3) Step iii: Synthesis of LA-EG_n-Cyclooctyne

LA-EG_{11}-cyclooctyne: LA-EG_{11}-NH_2 (0.1448 g, 0.1975 mmol), DCC (0.0489 g, 0.237 mmol) and the cyclooctyne-glyconic acid (0.0360 g, 0.1975 mmol) were dissolved in DCM (10 mL) and stirred at 0˚C under a nitrogen environment. A solution of DMAP (0.0050 g, 0.0395 mmol) in DCM (10 mL) was then added slowly over a period of 5-10 minutes. The mixture was stirred for 1 hour at 0˚C and then allowed to warm up to RT and stirred for a further 8 hours. The reaction mixture was filtered and washed with a small amount of DCM three times. The desired product was purified by silica gel column chromatography (MeOH:$CHCl_3$ = 7:93 v/v). The desired LA-EG_{11}-cyclooctyne was isolated as a yellow oil in 43% yield (0.0755 g, 0.0842 mmol). **TLC:** (MeOH/$CHCl_3$ 7 %: 93 %) R_f = 0.13. **^{1}H-NMR** (400 MHz, $CDCl_3$): 6.80 (s, br, 1H), 6.19 (s, br, 1H), 4.21 – 4.13 (m, 1H), 3.99 (d, J = 15.1 Hz, 1H), 3.80 (d, J = 15.1 Hz, 1H), 3.61 – 3.51 (m, 4H), 3.50 (m, 2H), 3.40 (m, 2H), 3.08 (m, 2H), 2.39 (m, 1H), 2.12 (m, 2H), 1.84 (m, 1H), 1.62 (m, 4H), 1.39 (m, 2H), 2.3 - 1.3 (m, 10H, ring). **^{13}C-NMR** (125 MHz, $CDCl_3$): δ 172.1 (C, C_{35}), 149.6 (C, C_{10}), 94.6 (C, C_2), 73.1 (C, C_8), 70.6 – 69.7 (20C, C_{13}-C_{33}), 56.4 (C, C_{40}), 49.2 (C, C_9), 42.2 (C, C_{34}), 40.2 (C, C_{41}), 39.1 (C, C_{11}), 38.5 (C, C_{42}), 36.3 (C, C_{39}), 34.7 (C, C_{36}), 34.3 (C, C_3), 34.0 (C, C_6), 29.7 (C, C_7), 29.6 (C, C_4), 28.9 (C, C_{38}), 25.4 (C, C_{37}), 20.7 (C, C_5). **IR**: 3323.50; 2924.19; 2854.80; 1644.98; 1533.60; 1447.78; 1098.83 cm^{-1} **MS**: calcd *m/z* for $C_{42}H_{76}N_2O_{14}S_2Na$ $[M + Na]^+$ = 919, found 919.70.

LA-EG_3-cyclooctyne: LA-EG_3-NH_2 (1.4117 g, 3.709 mmol), DCC (0.842 g, 4.08 mmol) and DMAP (0.0725 g, 0.594 mmol) were dissolved in dry DCM (20 mL). The mixture was then cooled to 0˚C in an ice bath while

under N_2. $C_{10}H_{14}O_3$ compound (0.676 g, 3.709 mmol) in 4 mL of DCM was slowly added through a syringe over 20 minutes under a nitrogen atmosphere. After addition, the reaction was left stirring at 0˚C for 1 hour and then was allowed to warm up gradually to RT and stirred for further 24 hours. The crude product was filtered and the solid washed with chloroform. The combined filtrate and washings were then evaporated and the product was purified by using silica gel column chromatography (MeOH: CH_2Cl_2 1:16 v/v). The eluted solutions were checked by TLC and the desired pure fractions LA-EG_3-cyclooctyne were combined. After evaporation of solvent, the desired product was obtained as a yellow oil in 26% yield (0.5375 g, 0.9866 mmol). TLC: (MeOH/CH_2Cl_2 1:16) R_f 0.29. ^{1}H-NMR (400 MHz, $CDCl_3$): δ 6.80 (s, br, 1H), 6.12 (s, br, 1H), 4.18 (s,1H), 3.64-4.01 (m,2H), 3.36-3.59 (m, 14H), 3.11 (m, 1H), 3.10 (m, 1H), 2.41 (m,1H), 2.09-2.40 (m, 4H), 1.19-2.07 (m, 20H). ^{13}C-NMR (100 MHz, $CDCl_3$): δ 169.7 (C, C_{19}), 128.5 (C, C_{10}), 73.2 (C, C_8), 70.6 – 69.9 (5C, C_{13}-C_{17}), 68.4 (C, C_2), 56.5 (C, C_{24}), 49.2 (C, C_9), 42.2 (C, C_{18}), 40.3 (C, C_{25}), 39.2 (C, C_{11}), 38.5 (C, C_{26}), 36.4 (C, C_{23}), 34.7 (C, C_{20}), 34.3 (C, C_3), 34.3 (C, C_6), 29.7 (2C, C_4,C_7), 28.9 (C, C_{22}), 25.4 (C, C_{21}), 20.7 (C, C_5). IR: 3325.56; 2925.14; 2851.31; 1654.91; 1533.75; 1446.65; 1098.83 cm^{-1} MS: calcd *m/z* for $C_{26}H_{46}N_2O_6S_2$ [M+H$^+$] = 546, found 546.0.

2.4) Steps iv & v: Synthesis of 1-azido-3,6-dioxaoct-8-yl 3,4,6-tri-*O*-acetyl-2-*O*-(2,3,4,6-tetra-*O*-acetyl-α-D-manno-pyranosyl)-α-D-mannopyranoside (2)

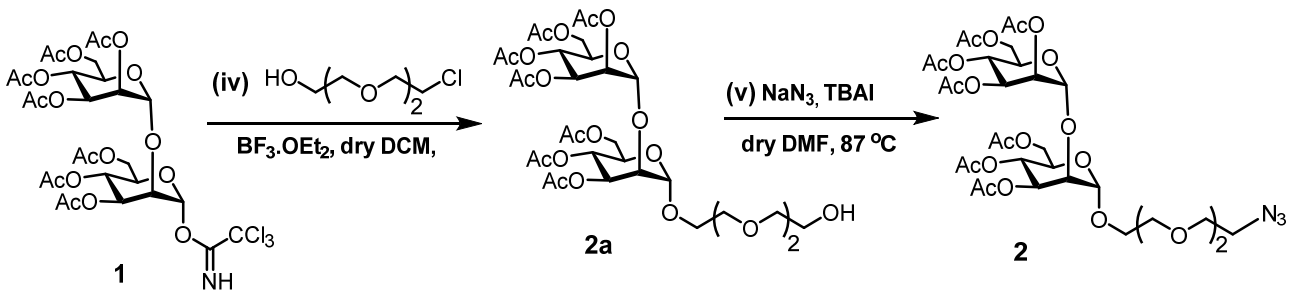

Step iv: 3,4,6-Tri-*O*-acetyl-2-*O*-(2,3,4,6-tetra-*O*-acetyl-α-D-mannopyranosyl)-α-D-mannopyranosyl trichloroacetimidate **1** (82 mg, 0.11 mmol) was co-evaporated with toluene several times before adding molecular sieves 4 Å (50 mg), anhydrous DCM (1 mL) and 2-[2-(2-chloroethoxy)ethoxy]ethanol (279 µL, 1.5 mmol). The resulting mixture was stirred at RT under a N_2 atmosphere for 1.5 h, and cooled to -50 °C. Freshly distilled BF_3·OEt_2 (14 µL, 0.11 mmol) was added to the reaction mixture, which was stirred at low temperature and slowly warmed up to 2 °C, over 2.5 h. The reaction mixture was washed with sat. aq. $NaHCO_3$ (2 × 2 mL), followed by brine (2 mL). The combined organic phase was dried over $MgSO_4$, and concentrated to leave crude yellow oil, which was purified by Biotage® flash column chromatography (Redisef®Rf 24 g silica column, hexane: EtOAc (0% EtOAc (1 col. vol.) → 0-70% EtOAc (over 12 col. vol.) → 70% EtOAc (over 12 col. vol.) to give a partially purified product (**2a**) which was directly used in the next step synthesis without further purification and characterisation.

Step v: The partially purified compound (**2a**) was dissolved in anhydrous DMF (3.5 mL) into which sodium azide (32 mg, 0.1 mmol) and TBAI (37 mg, 0.1 mmol) were added. The resulting reaction mixture was then stirred at 87 °C for 17 h. The reaction mixture was cooled to r.t., concentrated, and purified by Biotage® flash

column chromatography (Redisef®Rf 24 g silica column, Hexane:EtOAc (0% EtOAc (1 col. vol.) → 0-70% EtOAc (over 12 col. vol.) → 70% EtOAc (over 12 col. vol.) to give compound **2** as a colourless oil (43 mg, overall yield 49% over 2 steps); R_f 0.30 (3:7 Hexane–EtOAc); $[\alpha]_D^{25}$ 27.2 (c, 1.0, $CHCl_3$); **^{1}H NMR** (500 MHz, $CDCl_3$) δ_H; 5.40 (dd, 1H, $J_{3b,4b}$ 9.9 Hz, $J_{2b,3b}$ 3.6 Hz, H-3b), 5.36-5.23 (m, 4H, H-2b, H-3a, H-4a, H-4b), 4.97 (d, 1H, $J_{1a,2a}$ 2.0 Hz, H-1a), 4.91 (d, 1H, $J_{1b,2b}$ 1.9 Hz, H-1b), 4.21 (dd, 2H, $J_{6,6'}$ 12.1 Hz, $J_{5,6=5,6'}$ 4.9 Hz, H-6, H-6′), 4.12 (m, 3H, H-5b, H-6, H-6′), 4.04 (bs, 1H, H-2a), 4.01-3.95 (m, 1H, H-5a), 3.81 (m, 1H, C$\underline{H}_2$O), 3.70-3.60 (m, 9H, C$\underline{H}_2$O), 3.37 (t, 2H, *J* 5.1 Hz, C$\underline{H}_2$-N), 2.14 (s, 3H, C(O)C$\underline{H}_3$), 2.13 (s, 3H, C(O)C$\underline{H}_3$), 2.07 (s, 3H, C(O)C$\underline{H}_3$), 2.06 (s, 3H, C(O)C$\underline{H}_3$), 2.02 (s, 3H, C(O)C$\underline{H}_3$), 2.01 (s, 3H, C(O)C$\underline{H}_3$), 1.99 (s, 3H, C(O)C$\underline{H}_3$); **^{13}C NMR** (75 MHz, $CDCl_3$) δ_C; 171.0, 170.6, 170.5, 170.0, 169.8, 169.6, 169.5 (7 × C=O), 99.3 ($J_{C,H}$ 173.3 Hz, 5.1 Hz, α, C-1b), 98.5 ($J_{C,H}$ 171.6 Hz, α, C-1a), 77.2 (C-2a), 70.9, 70.8 (2 × $\underline{C}H_2O$), 70.4 (C-3a), 70.2 (2 × $\underline{C}H_2O$), 69.9 (C-2b), 69.3 (C-5b), 68.6 (C-3b), 69.5 (C-5a), 67.6 (ManO$\underline{C}H_2$), 66.5, 66.3 (C-4a, C-4b), 62.6, 62.2 (C-6a, C-6b), 50.8 ($\underline{C}H_2$-N), 21.0, 20.8, 20.8 (7 × O$\underline{C}H_3$); **IR** (ν_{max}/cm^{-1}): 2107 (N_3), 1744 (C=O); **HRMS:** Found $[M+Na]^+$ 816.2660, $C_{32}H_{47}N_3NaO_{20}$ requires 816.2645.

The corresponding ^{1}H and ^{13}C NMR spectra of compound **2** in $CDCl_3$ are shown below:

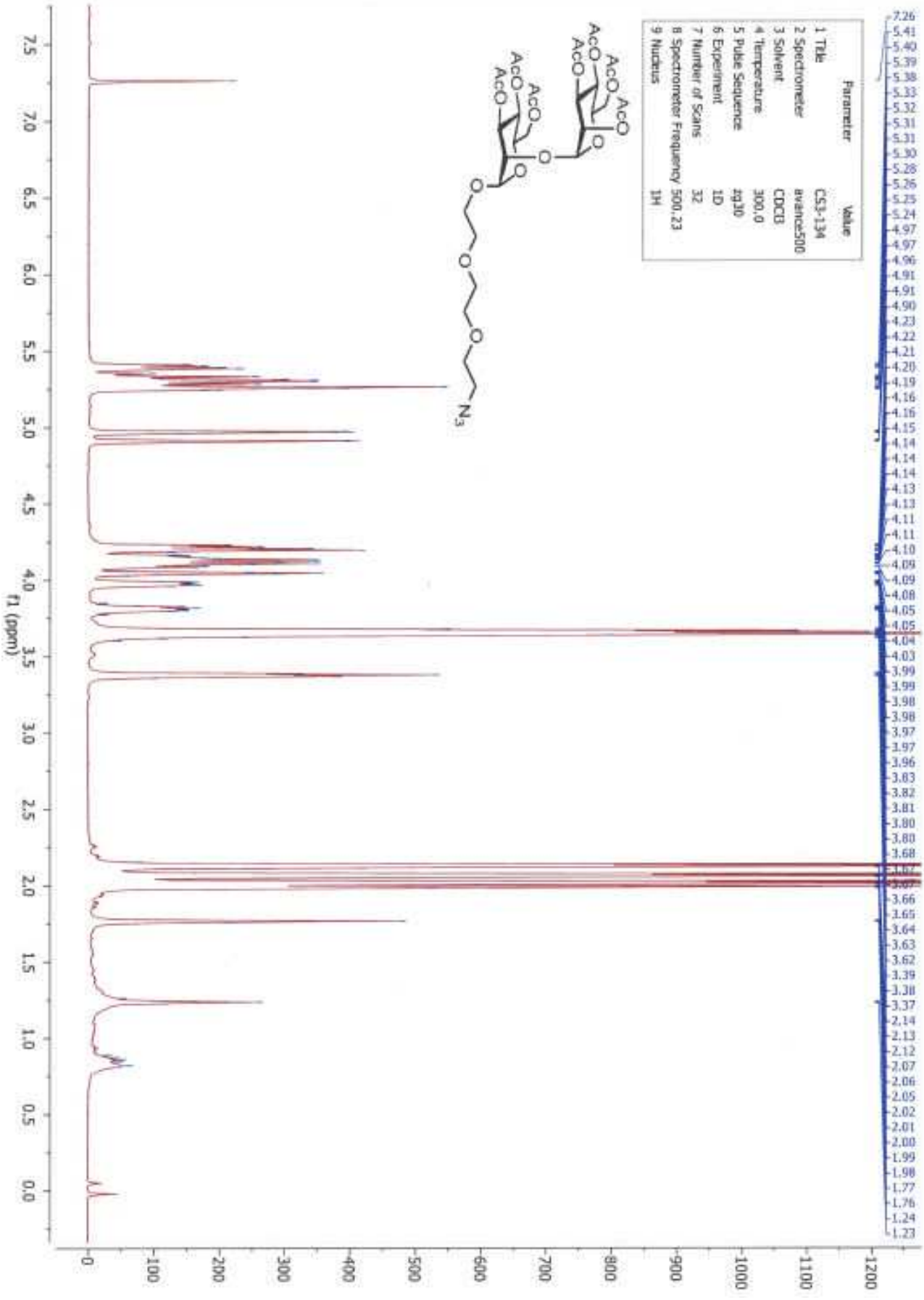

The ^{1}H-NMR spectrum of compound **2** in $CDCl_3$

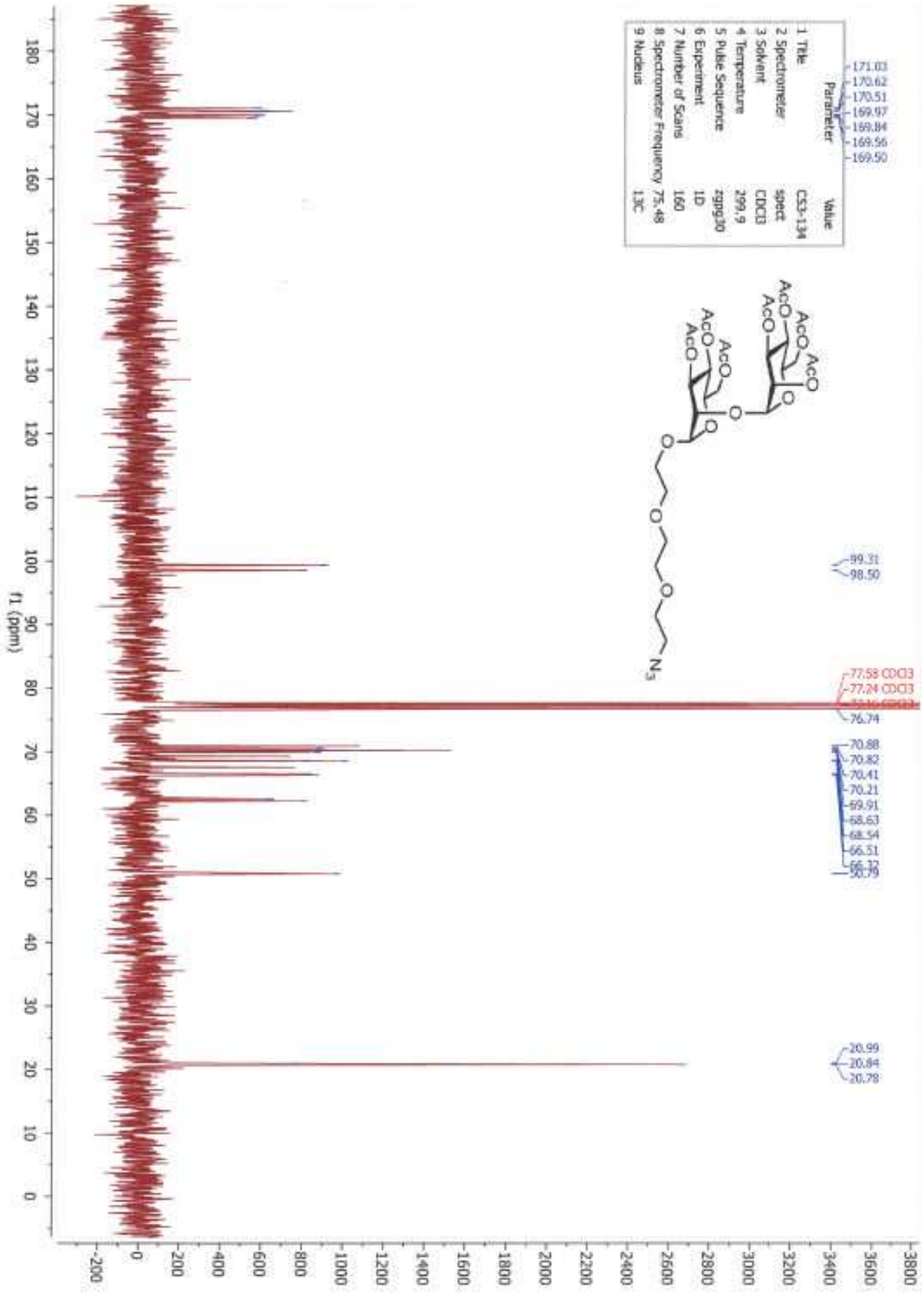

The ^{13}C-NMR spectrum of compound **2** in $CDCl_3$

2.5) Step vi: Synthesis of 1-Azido-3,6-dioxaoct-8-yl-2-*O*-α-D-mannopyranosyl-α-D-mannopyranoside (3)

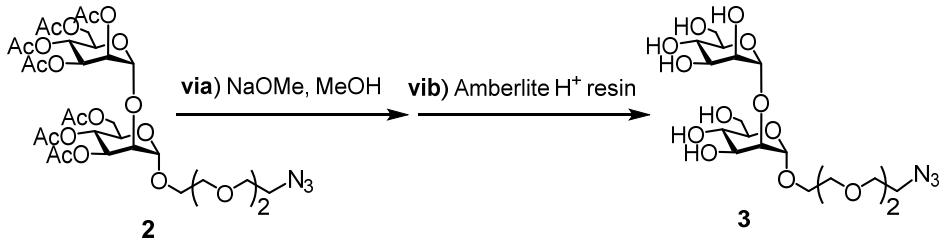

Sodium methoxide (5.3 mg, 0.10 mmol) was added to a solution of 1-azido-3,6-dioxaoct-8-yl 3,4,6-tri-*O*-acetyl-2-*O*-(2,3,4,6-tetra-*O*-acetyl- α-D-mannopyranosyl)-α-D-mannopyranoside **2** (38 mg, 0.05 mmol) in anhydrous MeOH (1 mL). After stirring for 17 h at r.t., the reaction mixture was neutralised with Amberlite® IRC 86 H^+ resin, filtered and concentrated to afford compound **3** (22 mg, 90%) as a colourless oil; R_f 0.38 (6:4:1 Chloroform–MeOH–H_2O); $[\alpha]_D^{21}$ 0.94 (C, 0.1, H_2O); δ_H (500 MHz, D_2O); 5.14 (d, 1H, $J_{1a,2a}$ 1.7 Hz, H-1a), 5.05 (d, 1H, $J_{1b,2b}$ 1.7 Hz, H-1b), 4.09 (dd, 1H, $J_{2b,3b}$ 3.4 Hz, $J_{1b,2b}$ 1.7 Hz, H-2b), 4.01 (dd, 1H, $J_{2a,3a}$ 3.4 Hz, $J_{1a,2a}$ 1.7 Hz, H-2a), 3.95 (dd, 1H, $J_{3a,4a}$ 9.2 Hz, $J_{2a,3a}$ 3.4 Hz, H-3a), 3.93-3.84 (m, 4H, H-3b, H-6, H-6′, C$\underline{H}_2$O), 3.82-3.61 (m, 15H, C-4a, C-4b, C-5a, C-5b, C-6, C-6′, C$\underline{H}_2$O), 3.55-3.51 (t, 2H, *J* 4.87 Hz, C$\underline{H}_2$-N); δ_C (75 MHz, D_2O); 102.3 ($J_{C,H}$ 171.3 Hz, 4.1 Hz, α, C-1b), 98.4 ($J_{C,H}$ 172.2 Hz, α, C-1a), 78.6 (C-2a), 73.3, 72.8, 66.6, 61.1 (2 × C-4, 2 × C-5), 70.3, 70.2 (C-3b), 69.9 (C-2b), 69.6 (C-3a), 69.5, 69.5, 69.3, 66.9 (4 × $\underline{C}H_2O$), 60.9, 50.2 (2 × C-6); **IR** (ν_{max}/cm^{-1}): 3331 (OH), 2103 (N_3); **HRMS:** Found $[M+NH_4]^+$ 517.2372, $C_{18}H_{37}N_4O_{13}$ requires 517.2352.

The corresponding ^{1}H and ^{13}C-NMR spectra of compound **3** are shown below:

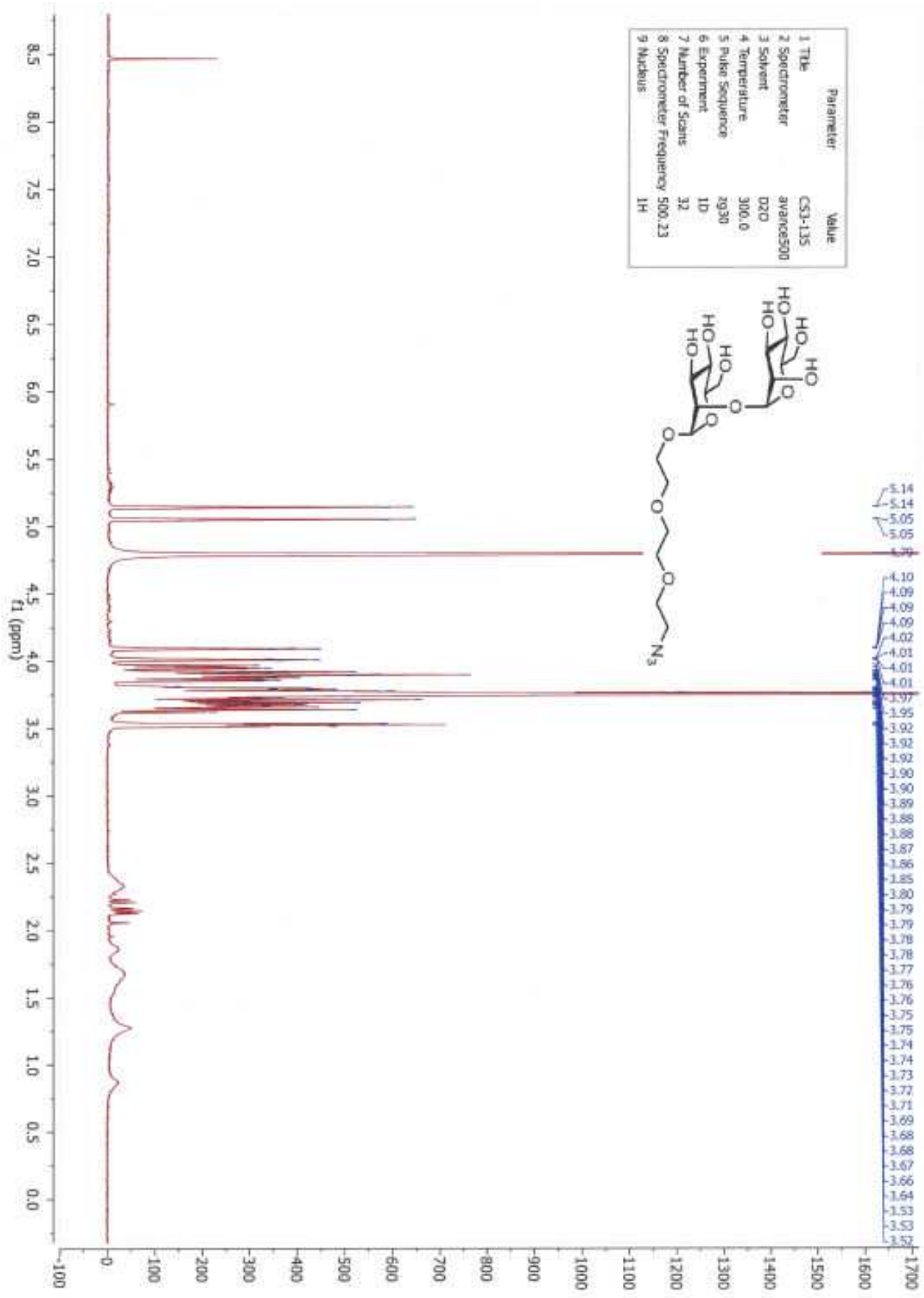

The ^{1}H-NMR spectrum of compound **2** in D_2O

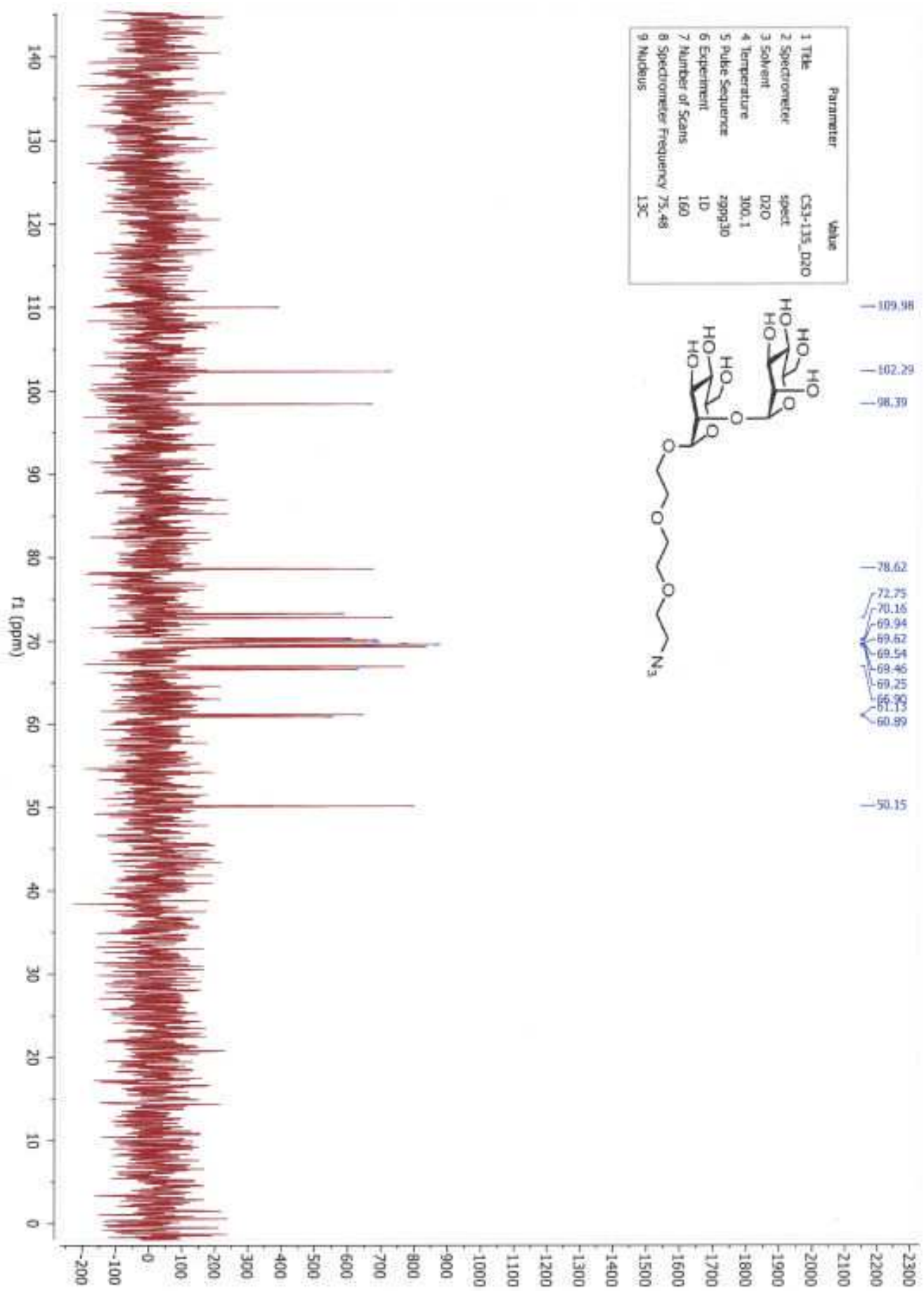

The ^{13}C-NMR spectrum of compound **2** in D_2O

2.6) Step vii/viii: Synthesis of DHLA-EG$_n$-DiMan (n =11 or 3)

LA-EG$_{11}$-cyclooctyne (0.050 M, 200µL, 10 µmole in ethanol) or LA-EG$_3$-cyclooctyne (0.10 M in ethanol, 100 µL, 10 µmole) was mixed with 1-azido-3,6-dioxaoct-8-yl-2-*O*- α-D-mannopyranosyl-α-D-manno-pyranoside (compound **3**, 0.100 M in methanol, 100 µL, 10 µmole) and allowed to react at RT for 48 h to form the corresponding LA-EG$_n$-DiMan ligands *via* copper-free click chemistry. Then tris(2-carboxyethyl)phosphine hydrochloride (TCEP.HCl, 12 mol µmole) in H_2O was added to the reaction mixture and incubated at RT for 30 min to reduce the ligands into its DHLA equivalents. After evaporation of solvent, the resulting DHLA-EG$_n$-DiMan ligand was purified by silica gel column chromatography using mixed chloroform and methanol solution (7:3, v/v) as eluting solvent. The fractions containing the desired ligands were collected and combined. The purity and chemical identity of the purified DHLA-EG$_n$-DiMan ligands were further confirmed by a LC-MS analysis. For DHLA-EG$_{11}$-DiMan**,** a single UV absorption band with a retention time of ~1.63 min from the LC elution profile was obtained which gave two MS peaks with m/z ratios of 1398.8 and 1420.7. The calculated MWs for $C_{60}H_{111}N_5O_{27}S_2$ ($[M+H]^+$) and $C_{60}H_{110}N_5O_{27}S_2Na$ ($[M+Na]^+$) are 1398.7 and 1420.7, respectively. A single UV absorption band in the LC eluting profile confirmed the high purify of the ligand.

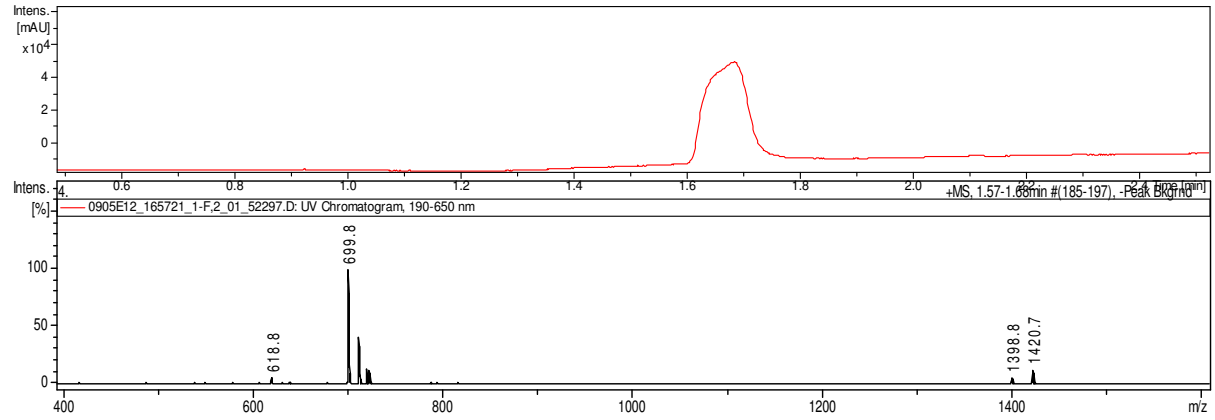

For DHLA-EG$_3$-DiMan, a single UV absorption band with a retention time of ~1.63 min from the LC elution profile was obtained, confirming its high purify. This fraction also gave two MS peaks with m/z ratios of 1046.6 and 1068.6. The calculated MWs for $C_{44}H_{79}N_5O_{19}S_2$ ($[M+H]^+$) and $C_{44}H_{78}N_5O_{19}S_2Na$ ($[M+Na]^+$) are 1046.2 and 1068.2, respectively. A single UV absorption band in the LC eluting profile confirmed the high purify of the ligand.

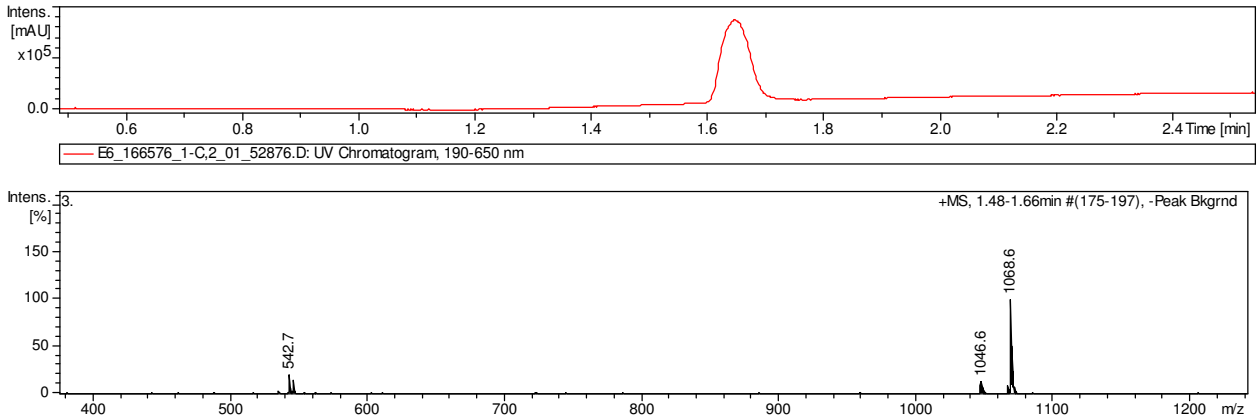

2.7) Synthesis of DHLA-zwitterion (DHLA-ZW)[1,6]

The synthesis of the DHLA-zwitterion spacer ligand was described in our previous publication. The crude product was further purified by HPLC. ^{1}H NMR (300 MHz, D_2O): δ (ppm) 3.60-3.70 (m,1H), 3.40-3.50 (m, 2H), 3.28-3.35 (m, 2H), 3.20-3.28 (m, 2H), 3.10-3.20 (m, 2H), 3.10 (s, 6H), 2.90 (t, 2H), 2.40-2.50 (m, 1H), 2.20 (t, 2H), 2.15 (m, 2H), 1.93-2.0 (m, 2H), 1.70 (m, 1H), 1.50-1.60 (m, 4H), 1.35-1.40 (m, 2H).

3: Preparation of QD-EG$_n$-DiMan and QD-EG$_n$-Man

3.1) CdSe/ZnS core/shell QD (λ_{EM} = 560 nm, 1 nmol) was precipitated by EtOH and re-dissolved in chloroform to remove any unbound free ligands as described previously.[7] Then DHLA-EG$_n$-DiMan ligand (n = 11 or 3, 800 nmol in $CHCl_3$), after deprotonation of its thiol groups by 0.10 M NaOH in EtOH (960 nmol), was added to the QD solution together with some extra methanol to make a homogenous solution. The reaction mixture was stirred at RT in darkness for 30 min. After which the QD-glycan conjugates were precipitated by adding hexane. The resulting cloudy mixture was centrifuged at 10,000 × g for 5 min, where all the QDs pelleted, leaving the supernatant colourless. After careful removal of the supernatant, the QD pellet was dissolved in 100 µL of pure H_2O. The QD solution was then transferred to a 30 KD MWCO spin column and washed with H_2O (100 µL× 3) to remove any unbound free ligands to yield the QD-EG$_n$-DiMan stock. Its concentration was determined by measuring its absorbance at 546 nm (the first exciton peak absorption) using the Beer-Lambert law and a QD molar extinction coefficient of 1.3×10^5 $M^{-1}\cdot cm^{-1}$.[7,8]

3.2) Determination of carbohydrate ligand loading on the QDs

The amount of the glycan ligand loaded on the QD was determined by phenol-sulfuric acid method. First, the DHLA-EG$_n$-DiMan (n=11 or 3) stock in H_2O (1.55 or 0.95mg/mL respectively) was mixed with 5% phenol in H_2O and sulphuric-acid to generate a calibration curve. To a solution of DHLA-EG$_n$-DiMan in H_2O (62.5 µL), 62.5 µL of 5% phenol in H_2O followed by 312.5 µL of concentrated H_2SO_4 was added. The mixture was vortexed and allowed to stand at RT for 30 min. The absorbance of the solution at 490 nm was measured against a blank pure water control solution to generate a calibration curve as follow:

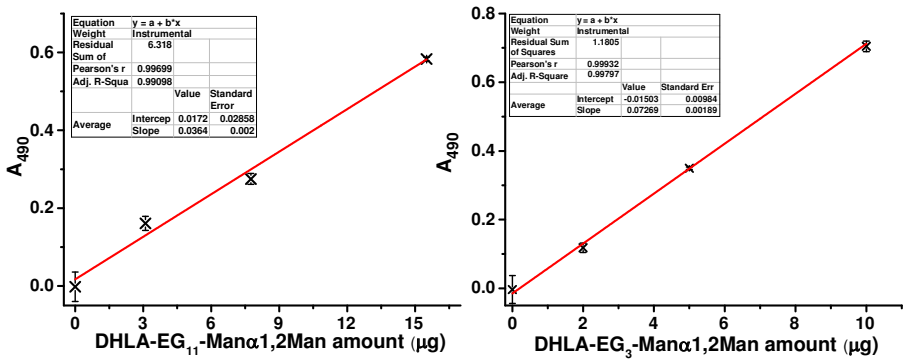

The unconjugated DHLA-EG$_n$-DiMan ligands collected from the clear supernatant (after removal of organic solvent and dissolving in H_2O) and spin column filtrate were combined to make a total volume of 594 µL for DHLA-EG$_{11}$-DiMan and 564 µL for DHLA-EG$_3$-DiMan. The 2 µL (for DHLA-EG$_{11}$-DiMan) or 4 µL (for DHLA-EG$_3$-DiMan) of the solution was then mixed with H_2O to make up to a final volume of 62.5 µL. Phenol and H_2SO_4 were then added as above to determine the amounts of unconjugated mannose ligand. The dilution

factors were then corrected to calculate the total amount of unconjugated ligands. Assuming the difference between the amounts of ligand added and unconjugated were those have bound to the QD, the average number of DHLA-EG_n-DiMan molecules conjugated to each QD was then calculated as 281±25 and 369±38 for n = 11 and 3, respectively. Using the same method, the number of DHLA-EG_n-Man ligands conjugated onto each QD was determined as 222 ±62 and 330±70 for n=11 and 3, respectively.

4: Protein Production and Labeling

The soluble extracellular segments of DC-SIGN and DC-SIGNR (abbreviated as DC-SIGN and DC-SIGNR hereafter) which are known to form stable homotetramers and faithfully retain their native glycan binding properties was used to study tetrameric protein-QD-carbohydrate interaction here.[9,10] The proteins were expressed in *E. coli.,* purified by Man-Sepharose affinity column in elution buffer (25 mM Tris pH 7.8, 1.25M NaCl, 2.5 mM EDTA). Proteins were then dialysed against 10 mM Tris pH7.8, 100 mM NaCl, 2.5mM EDTA and further purified by size exclusion chromatography (30 × 1 cm Superdex 200 column, Amersham Bioscience) eluted with 10 mM Tris pH7.8, 100 mM NaCl, 2.5 mM EDTA at a flow rate of 0.3 ml/min (see the eluting profile below[1]).

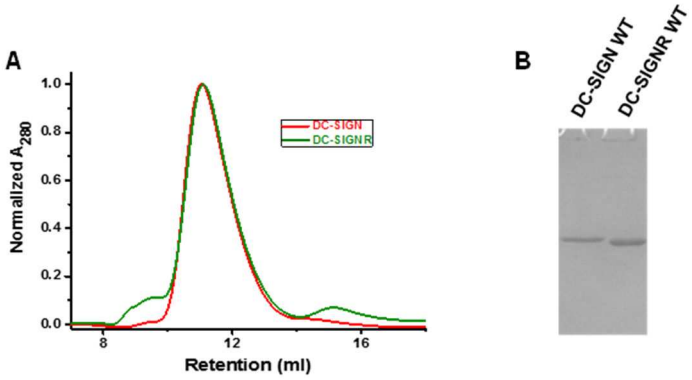

(A): Size exclusion chromatography graph of extracellular segment of DC-SIGN and DC-SIGNR. The dominant peaks eluted out at ~11.5 ml correspond to the desired tetrameric proteins. (**B):** SDS-polyacrylamide gel electrophoresis of proteins following purification, only a single band was found for each protein. The gel (17.5% polyacrylamide) was stained with coomassie blue.

The mutant proteins, DC-SIGN-Q274C and DC-SIGNR-R287C, were constructed by using site-directed mutagenesis on the CRD for site-specific labeling. The selected mutation site sits away from the sugar binding sites to avoid interfering with its glycan binding property. Proteins were expressed in *E. coli.,* purified by Man-Sepharose affinity column and labeled with Atto594-maleimide as described previously.[1] The average labeling ratio of Atto594 dye on each CRD was found to be 0.80 for DC-SIGN-Q274C and 0.76 for DC-SIGNR-R287C.

Monomeric DC-SIGN and DC-SIGNR CRDs were expressed from *E.coli.,* purified and labeled with 3-4 mol equivalent Atto594-NHS ester. The average dye labeling ratio on each CRD was found to be ~2.

All labeled proteins were further purified by Man-Sepharose affinity column to remove any unreacted free dye molecules. It also confirmed that the man-binding ability of the proteins was retained after the labeling.

5: FRET Measurements

5.1) Fluorescence spectra were recorded on a Cary Eclipse Fluorescence Spectrophotometer using a 0.70 mL quartz cuvette (λ_{EX} = 450 nm, corresponding to the minimum absorption of the Atto594 to minimize the direct excitation background) over 480-800 nm. All measurements were done in the binding buffer (20 mM HEPES pH 7.8, 100 mM NaCl, 10 mM $CaCl_2$) containing 10 μg/mL of a His_6-Cys peptide which was found to increase the QD stability and reduce non-specific adsorption.[1,2] The labeled proteins were mixed with the QD at room temperature for 20 min before fluorescence spectra were recorded. Binding of labeled monomeric DC-SIGN CRD or DC-SIGNR CRD with the QD-DiMan was performed in the same way as described previously.[1] Other DC-SIGN/R-QD-EG_{11}-DiMan binding studies were performed as follows:

Apparent K_d measurement: systematically varying concentrations of Atto594 labeled DC-SIGN or DC-SIGNR and QD-EG_n-glycan conjugates (n =3 or 11, glycan = Man or DiMan) were mixed under a fixed protein:QD molar ratio (PQR) of 1:1 for DC-SIGN or 10:1 for DC-SIGNR in the binding buffer containing 1 mg/ml BSA to reduce any nonspecific absorption of the QD and proteins on surfaces. The samples were incubated at room temperature for 20 min before fluorescence spectra were recorded. Adjustments of the PMT voltages and EX/EM slit widths were used to compensate the low fluorescence signal at low concentrations. The protein only background in the absence of the QD under identical experiment conditions was also recorded and subsequently corrected from the resulting fluorescence spectra.

5.2) Calcium dependent binding: the Atto-594 labeled DC-SIGN in buffer (20 mM HEPES, 100 mM NaCl, 2.5 mM EDTA, pH 7.8) was dialysed extensively against a calcium free buffer (20 mM HEPES, 100 mM NaCl, pH 7.8) to remove EDTA. Then the labeled protein (final $C_{protein}$ = 0.2 μM) was mixed with QD-EG_n-DiMan (final C_{QD} = 20 nM) in calcium free buffer containing His_6-Cys (10 μg/mL). Different amount of calcium was then added to the mixture and incubated at room temperature for 20 min before measurement. As above, the protein only background spectra were also recorded and subsequently corrected from the resulting fluorescence spectra.

5.3) Unlabeled protein competition assay: different amounts of the wild type DC-SIGN or DC-SIGNR was mixed with a fixed amount of Atto-594 labeled DC-SIGN first in binding buffer before being added to the QD-EG_n-DiMan or DHLA-zwitterion diluted QD-EG_n-DiMan containing 25% glycan density. The labeled DC-SIGN:QD molar ratio (PQR) was fixed at 12.5 in all experiments. The samples were incubated at room temperature for 20 min before their fluorescence spectra were recorded.

5.4) Correlation between FRET ratio and QD bound proteins[2]. For a single QD donor which is in FRET interaction with ***N*** identical acceptors (*e.g.* under idential QD-dye distance *r*), the FRET efficiency, *E*, can be given in the following equation:

$$E = N \times R_0^6/[N \times R_0^6 + r^6] = 1/[1 + (r/R_0)^6/\mathrm{N}] \quad (1)$$

where R_0 is the Förster radius of the QD-single dye FRET pair and *r* is donor-acceptor distance. *E* can also be measured *via* the enhanced acceptor emission by the following equation:

$$E = I_{Dye}/[I_{Dye} + \gamma \times I_{QD}] = 1/[1 + \gamma \times I_{QD}/I_{Dye}] \quad (2)$$

Where γ is a correcting factor for the different dye and QD fluorescence quantum yield. Assuming that the shape of the QD and dye fluorescence spectra are independent of their intensity, then the integrated I_{QD}/I_{Dye} ratio should be linearly propotional to the peak intensity ratio, *e.g.* $I_{QD}/I_{Dye} = \alpha\ I_{554}/I_{626}$.

The combination of equations (4) and (5) gives the following equation:

$$1/[1 + \gamma \times I_{QD}/I_{Dye}] = 1/[1 + \gamma \times \alpha \times I_{554}/I_{626}] = 1/[1 + (r/R_0)^6/N] \quad (3)$$

This yields the following relationship:

$$\gamma \times \alpha \times I_{554}/I_{626} = (r/R_0)^6/N \quad (4)$$

Therefore the following relationship is obtained:

$$I_{626}/I_{554} = N\ [\gamma \times \alpha \times (R_0/r)^6] \quad (5)$$

Where γ, α and R_0 are all constant values. This equation shows that the apparent FRET ratio I_{626}/I_{554} should increase linearly with ***N***, the number of acceptors (proteins) bound to each QD if all of the proteins were bound to the QD in the same distance (R_0/r value).

6: Dynamic Light Scattering and TEM Imaging

6.1) Dynamic Light Scattering

The hydrodynamic sizes of QD-EG_n-DiMan (n= 3 or 11) before and after binding to the unlabeled wild-type proteins were recorded on a Malvern ZETASizer-Nano using disposable polystyrene cuvette as before.[1] A total of 10 scans for each sample were recorded and the resulting size distributions were added up to produce the size distribution histogram. The histogram was then fitted by Gaussian function to determine the mean size and full-width at half-maximum (FWHM) for each sample.

6.1a) Estimation of the inter-DiMan distance (X)[11]

For a QD with a radius *r* and conjugated with *N* ligands, the footprint for each ligand on the QD surface is:

$$k = \frac{4\pi r^2}{N} \quad (6)$$

The average deflection angle for each ligand on the QD surface can be calculated by:

$$\theta = \frac{2\times 180\times\sqrt{\frac{k}{\pi}}}{r\pi} = \frac{229.3}{\sqrt{N}} \quad (7)$$

θ for QD-EG_3-DiMan and QD-EG_{11}-DiMan (*N* = 369 and 281) are thus calculated as 11.94 and 13.68°, respectively. The inter-glycan distance on the QD surface (X) can be calculated *via*:

$$X = 2 \times r \times sin(\frac{\theta}{2}) \quad (8)$$

Where *r* is hydrodynamic radius of the QD-DiMan measured by DLS (Figure S2), where *r* = 8.3/2 = 4.15 nm for QD-EG_3-DiMan and 9.5/2 = 4.75 nm for QD-EG_{11}-DiMan. Using these parameters, the inter-glycan spacing (X) are calculated as:

QD-EG_3-DiMan: X = 2 × 4.15 × sin(11.94/2) = 0.86 nm

QD-EG_{11}-DiMan: X = 2 × 4.75 × sin(13.68/2) = 1.13 nm.

6.2) TEM imaging

6.2.1) QD EDX analysis and TEM image collection:

Three samples: (1) QD-EG_{11}-DiMan, (2) QD-EG_{11}-DiMan + wild-type DC-SIGN and (3) QD-EG_{11}-DiMan + wild-type DC-SIGNR were prepared (final C_{QD} = 40 nM and $C_{protein}$=1.5 μM) in binding buffer (20 mM HEPES, pH7.8, 100 mM NaCl, 10 mM $CaCl_2$ and 10 μg/mL His_6-cys peptide the same as those used in FRET studies).

To analyse the dispersion of the QDs, TEM samples were prepared by plunge-freezing into liquid ethane followed by warming under vacuum to capture the QD dispersions in their native dispersed state as demonstrated in our previous paper.[12] Briefly, 3.5 μL of suspension was placed onto a plasma-cleaned TEM grid with a continuous carbon support film, blotted, and plunge frozen into liquid ethane. The TEM grids were then warmed to RT over several minutes by placing the specimens in the liquid nitrogen cooled storage container in a rotary pumped vacuum desiccator.

The samples were then analysed using an FEI Titan Cubed Themis 300 G2 S/TEM equipped with FEI SuperX energy dispersive X-ray (EDX) spectrometers. The samples were imaged using high angle annular dark field scanning transmission electron microscopy (HAADF STEM) mode,[13] which provides atomic number contrast (≈$Z^{1.7}$), thereby permitting imaging of the high atomic number quantum dots (brighter) on the low atomic number background (darker).

Images were collected for each sample, with EDX spectroscopy used for the QD-Mannose sample to confirm that the small nanoparticles imaged were indeed quantum dots. Cadmium, sulphur and selenium from the quantum dots was detected, with other peaks (carbon, oxygen, silicon, and copper) due to the microscope, TEM grid or support film. A series of images at the same magnification were recorded for each sample, allowing easy comparison of the nanoparticle dispersion state of the three samples.

EDX spectrum (right) collected from the circled QD (left) from **Sample 1:** QD-EG_{11}-DiMan

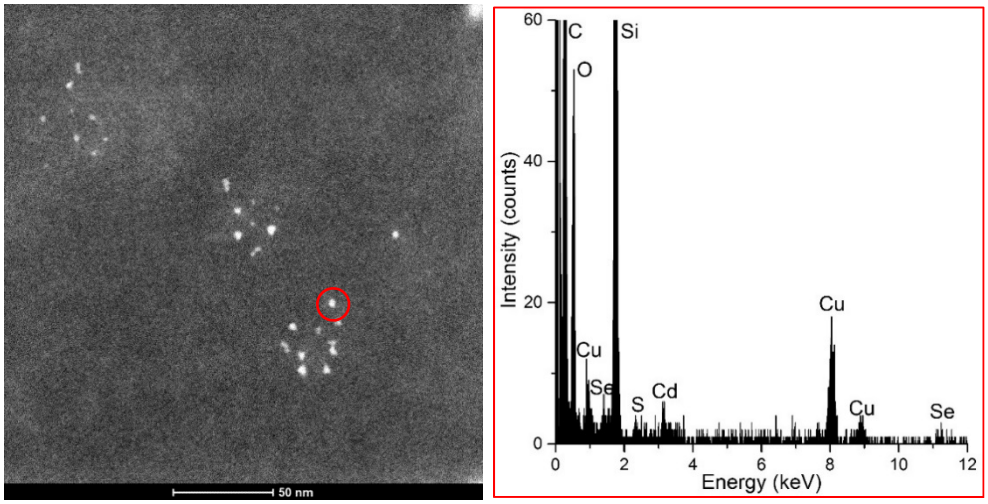

6.2.2) Comparison of QDs in Dispersion State

Sample 1: QD-EG_{11}-DiMan in binding buffer

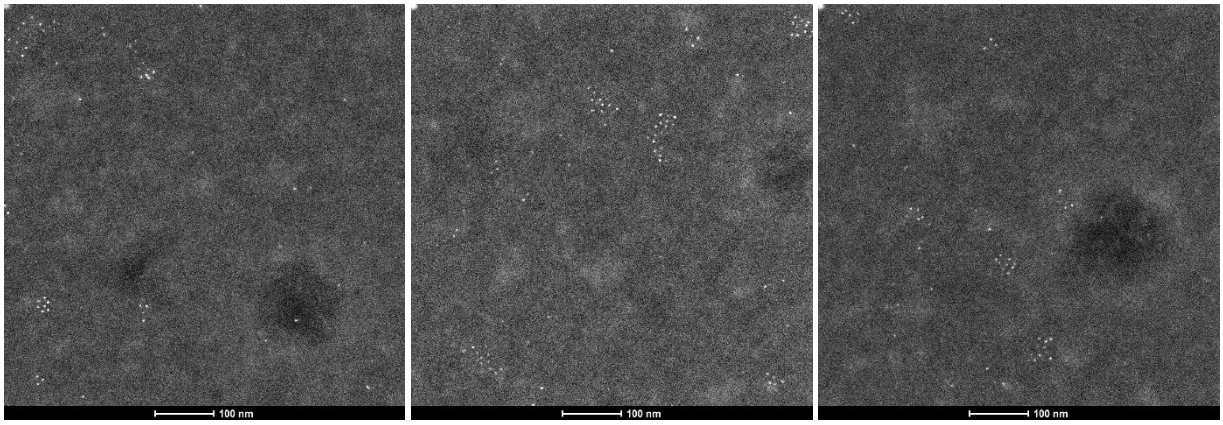

Sample 2: QD-EG_{11}-DiMan + DC-SIGN in binding buffer

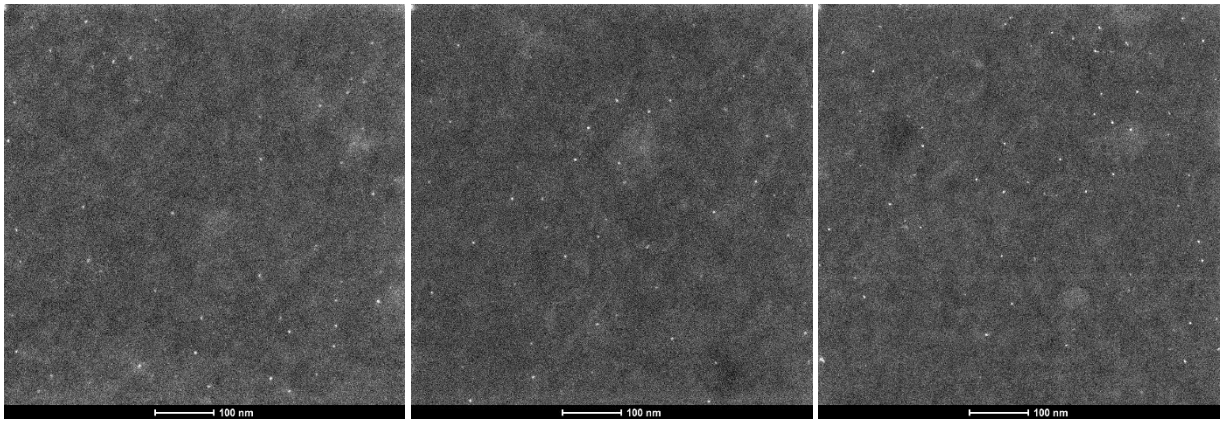

Sample 3: QD-EG_{11}-DiMan + DC-SIGNR in binding buffer

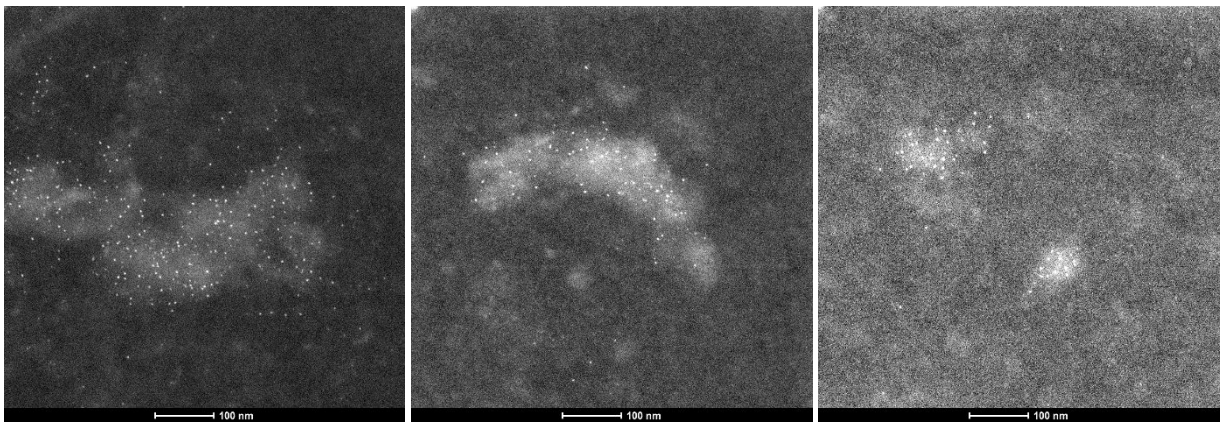

6.2.3) Measurement of Nearest Neighbour Distances

HAADF STEM images recorded above of the three QD samples were analysed in MATLAB in order to measure the nearest neighbour distances.

Sample 1	QD-EG_{11}-DiMan	5 images	210 QDs
Sample 2	QD-EG_{11}-Man +DC-SIGN	10 images	464 QDs
Sample 3	QD-EG_{11}-Man +DC-SIGNR	10 images	837 QDs

Histograms of nearest neighbour distances were produced for each image, and for the combined images for each sample (in this case shown as a percentage of the population to overcome the effect of the different number of quantum dots measured in each sample).

7: QD Fluorescence Quenching Assay by GNP-EG_3-DiMan

7.1) Gold nanoparticle synthesis and DHLA-EG_3-DiMan conjugation

Gold nanoparticle (GNP) was synthesized by using the standard citrate reduction of the $H[AuCl_4]$ under reflux conditions as reported in a previous publication.[14] The resulting GNP has an average size of *ca.*15 nm as determined by the TEM imaging shown in **Figure S12**. The GNP stock concentration was determined by its absorbance at 524 nm using the Beer-Lambert law and an extinction coefficient of 9.21×10^8 $M^{-1}\cdot cm^{-1}$.[14]

For GNP-glycan conjugation, 0.4 nmol of the GNP was mixed 0.6 μmol of DHLA-EG_3-DiMan (ligand:GNP molar ratio ~1500 to ensure high glycan density, and the shorter EG_3 linker glycan was used to reduce distance and hence higher quenching efficiency) and stirred for overnight. The resulting reaction mixture was centrifuged at 13000 rpm for 15 min where the GNP pelleted, leaving the supernatant colourless. After careful removal of supernatant, the GNP pellet was re-suspended in H_2O or buffer to make the GNP-EG_3-DiMan stock. The GNP concentration was determined by its absorbance at 524 nm using the Beer-Lambert law using an extinction coefficient of 9.21×10^8 $M^{-1}\cdot cm^{-1}$.[14]

To study GNP-EG_3-DiMan stability in buffer. Pellet was dissolved in 20 mM HEPES pH7.8, 100mM NaCl, containing 10 mM $CaCl_2$. Its hydrodynamic size determined by DLS was effectively the same as that in pure water. This result suggests that the GNP-EG_3-DiMan is stable in binding buffer containing 10 mM $CaCl_2$ and shows no evidence of aggregation (see Figure S12).

7.2) Preparation of CdSe/ZnSe/ZnS core/shell/shell QD-EG_3-DiMan (λ_{EM} ~ 605 nm) and QD quenching evaluation

CdSe/ZnSe/ZnS core/shell/shell QD (λ_{EM} ~ 605 nm) was conjugated with DHLA-EG_3-DiMan using the same method as that described in part 3 for CdSe/ZnS core/shell QD using a QD:ligand molar ratio of 1:2000. Any unconjugated free DHLA-EG_3-DiMan ligand was removed as that described in part 3. The QD concentration was determined by measuring its absorbance at the first exciton peak at 589 nm using an extinction coefficient of 3.3×10^5 $M^{-1}\cdot cm^{-1}$.

For quenching experiment, the QD_{600}-EG_3-DiMan (final C_{QD} = 10 nM), GNP-EG_3-DiMan (final C_{GNP} = 5 nM) and protein (final concentration = 125 nM) were mixed in an Eppendorf tube in binding buffer (20 mM HEPES

pH7.8, 100 mM NaCl, 10 mM $CaCl_2$) containing 2.5 μg/mL His_6-Cys peptide. The experimental conditions were the same as those used in protein-QD binding assays described above. A protein: QD molar ratio of 12.5 was chosen to saturate the QD binding by the proteins as revealed by the FRET titration results (see Figure 1). The mixture was incubated at room temperature for 20 min before the fluorescence spectra were recorded (λ_{EX} = 585 nm, emission range over 590-650 nm).

8: Inhibition of viral entry

The effects of QD-EG_n-DiMan (n =11 or 3) on Ebola virus glycoprotein (EBOV-GP) driven entry into 293T cells were assessed by using our established procedures.[1] Briefly, 293T cells seeded in 96-well plates were transfected with plasmids encoding DC-SIGN or DC-SIGNR or control with empty plasmid (pcDNA). The cells were washed at 16 h post transfection and further cultivated at 37°C, 5% CO_2 in Dulbecco's modified eagle medium (DMEM) containing 10% fetal bovine serum (FBS). At 48 h post transfection, the cells were exposed to twice the final concentration of QD-DiMan inhibitor in DMEM supplemented with 10% FBS for 30 min in a total volume of 50 μl. Thereafter, the cells were inoculated with 50 μl of prepared MLV vector particles encoding the luciferase gene and bearing either EBOV-GP (which can use DC-SIGN/R for augmentation of host cell entry) or the vesicular stomatitis virus glycoprotein (VSV-G, which does not use DC-SIGN/R for augmentation of host cell entry). Under these conditions, binding of QD-DiMan to DC-SIGN/R on the surface of 293T cells can block EBOV-GP interactions with these lectins, which should result in reduced luciferase gene transduction efficiency and hence reduced cellular luciferase activity. At 6 h post inoculation, 100 μl of fresh DMEM culture medium was added and the cells incubated for another 72 h. Thereafter, luciferase activities in cell lysates were determined using a commercially available kit (PJK), following the manufacturer's instructions, as described in our previous publication.[1]

9) Supporting Tables

Table S1: Best fitting parameters derived from Hill fit of the QD-EG_n-glycan-DC-SIGN/R binding curves (**Figure 4**): $y = R_{max} \times x^n/(k_d^n + x^n)$, where R_{max} is the maximum I_{626}/I_{554} ratio, k_d is protein concentration that gives 50% of the R_{max} (*i.e.* apparent binding dissociation constant) and *n* is the Hill coefficient.

QD + protein	R_{max}	Apparent K_d (nM)	n	R^2
QD-EG_3-Man + DC-SIGN	3.3±0.3	35±7	0.76±0.02	0.9999
QD-EG_{11}-Man + DC-SIGN	2.1±0.1	714±18	0.81±0.03	0.9991
QD-EG_3-DiMan + DC-SIGN	0.41±0.01	0.61±0.07	0.45±0.03	0.9982
QD-EG_{11}-DiMan + DC-SIGN	2.09±0.09	2.1±0.5	0.56±0.03	0.9998
QD-EG_3-Man + DC-SIGNR	1.61±0.06	62±8	1.2±0.3	0.9987
QD-EG_{11}-Man + DC-SIGNR	1.69±0.07	633±77	1 (fixed)	0.9985

Table S2: Hydrodynamic diameters (D_h, nm) of the QD-EG_n-DiMan conjugates before (in pure water) and after (in binding buffer) binding with DC-SIGN or DC-SIGNR.

EG linker length	QD-EG_n-DiMan	QD-EG_n-DiMan + DC-SIGN	QD-EG_n-DiMan + DC-SIGNR	
			Peak 1	Peak 2
n=11	9.5±0.1	42.0±0.5	124±2	205±12
n=3	8.3±0.1	41.4±0.5	138±2	217±12

10) Supporting Figures

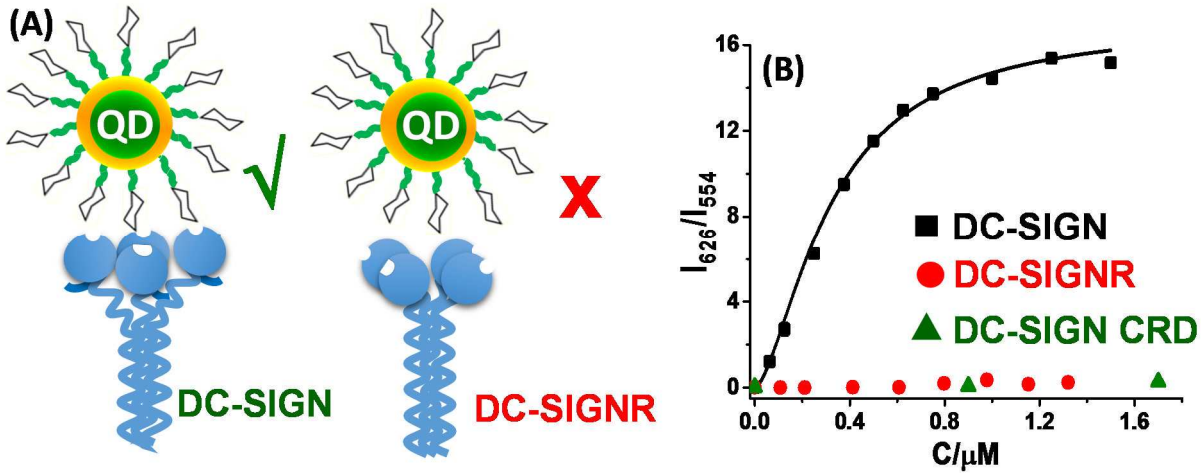

Figure S1. (A) Our previously proposed DC-SIGN/R-QD-EG$_n$-Man binding models: the CRDs are pointing uprightly in the same direction in DC-SIGN and so readily bind to multiple mannoses on the QD to give strong multivalent binding; whereas the CRDs are pointing sideway in different directions in DC-SIGNR, making them unable to bind simultaneously to multiple mannoses on the QD, resulting in weak/minimal binding. (**B**) Comparison of the apparent FRET ratio (I_{626}/I_{554}) as a function of protein concentration for DC-SIGN (black squares), DC-SIGNR (red dots) and monovalent DC-SIGN CRD (green triangles) binding to QD-EG$_3$-Man. The FRET signals resulting from DC-SIGNR and monovalent DC-SIGN CRD binding are equally weak and negligible.

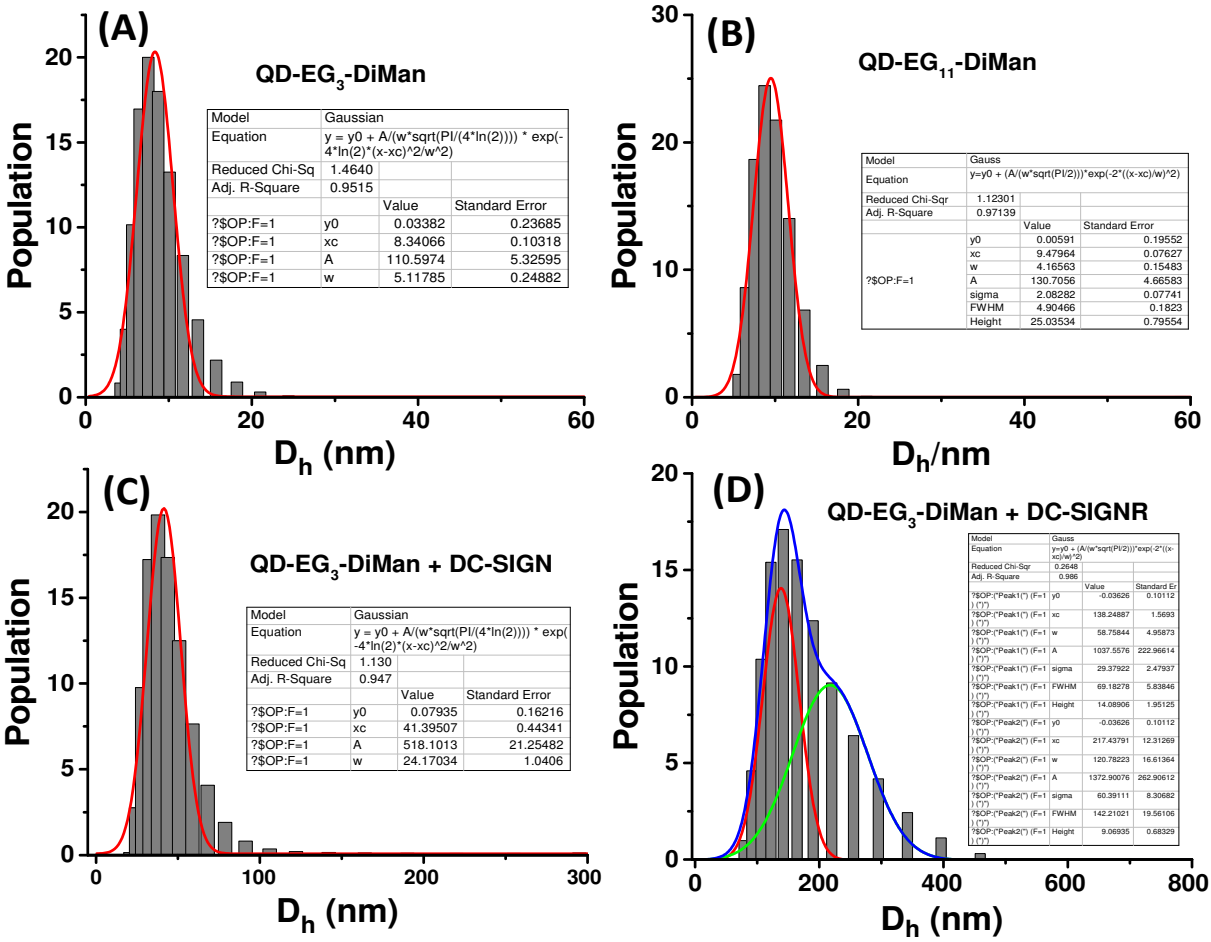

Figure S2: Hydrodynamic diameter (D_h) histograms of the QD-EG$_3$-DiMan (**A**) and QD-EG$_{11}$-DiMan (**B**) in pure H_2O measured by dynamic light scattering. (**C, D**) D_h histograms of QD-EG$_3$-DiMan after binding with DC-SIGN (**C**) or DC-SIGNR (**D**) in binding buffer at PQR =12.5. All data were shown in volume population.

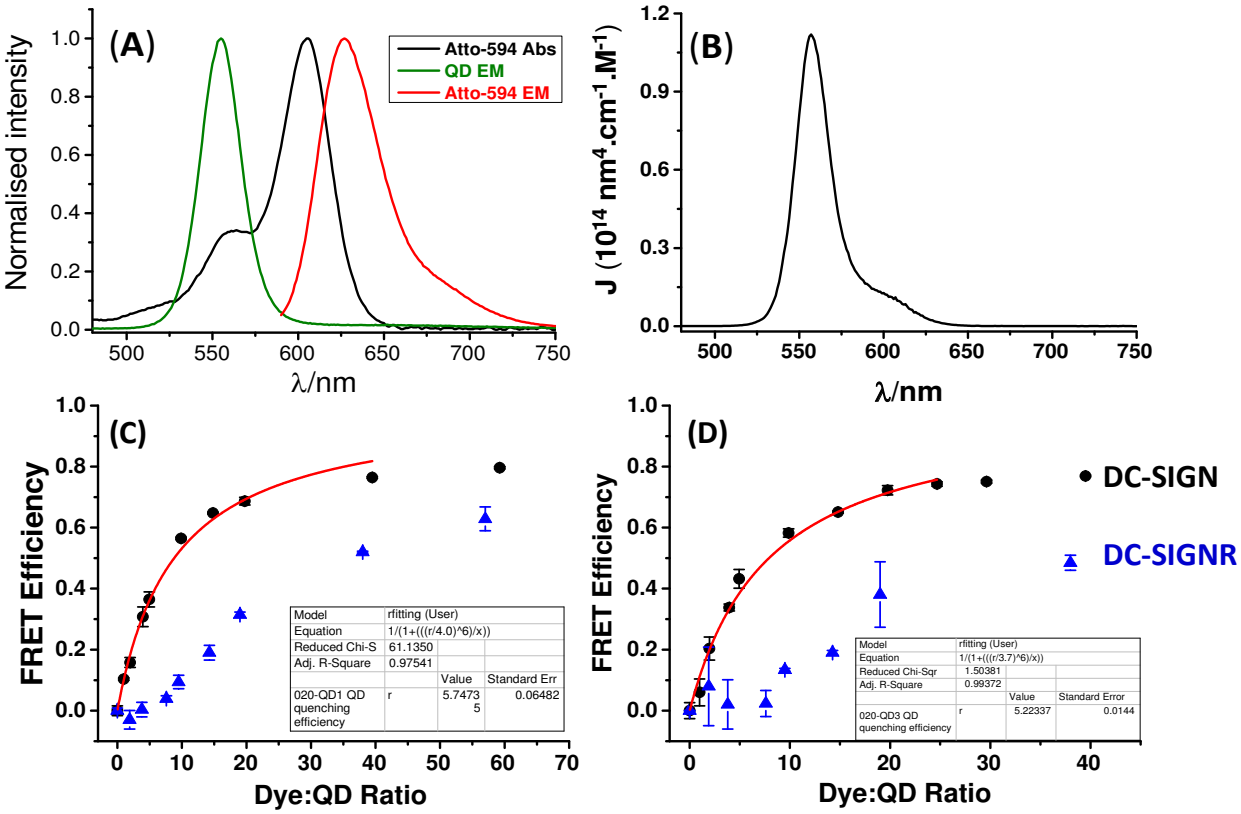

Figure S3. (**A**) Normalized fluorescence spectra of the QD (**green**) and Atto-594 (**red**) as well as the Atto-594 absorption spectrum (**black**). (**B**) Spectral overlap function ($J_{(\lambda)}$) of the QD-Atto-594 FRET pair. (**C, D**) Plots of FRET efficiency *versus* dye:QD molar ratio for QD-EG_{11}-DiMan (**C**) or QD-EG_3-DiMan (**D**) binding to DC-SIGN (black dots) or DC-SIGNR (blue triangles). The DC-SIGN binding data were fitted by a single QD donor in FRET interaction with *N* identical acceptors model, $E = 1/[1+(r/R_0)^6/N]$. Using a Förster radii (R_0) of 3.7 and 4.0 nm for QD-EG_3-DiMan/QD-EG_{11}-DiMan-Atto-594 FRET pair calculated below, the average QD-dye distance *r* for DC-SIGN binding to QD-EG_{11}-DiMan (**D**) and QD-EG_3-DiMan (**C**) are calculated to be ~5.7 and ~5.2 nm, respectively. However, the corresponding DC-SGNR binding data appear to be S-shaped and cannot be fitted by a single QD donor in FRET interaction with *N* identical acceptors model.

The spectral overlap function between QD emission and Atto-594 absorption was calculated *via*:

$$J_{(\lambda)} = \frac{\int PL_{D(\lambda)}\, \varepsilon_{A(\lambda)}\, \lambda^4\, d\lambda}{\int PL_{D(\lambda)} d\lambda}$$

Where $PL_{D(\lambda)}$ is the normalised QD fluorescence intensity at λ; $\varepsilon_{A(\lambda)}$ is the acceptor absorption coefficient at λ. The integral of the spectral overlap for the QD-Atto-594 pair: $I = 3.52 \times 10^{15}$ ($nm^4.cm^{-1}.M^{-1}$)

Using Rhodamine 6G in ethanol (QY = 95%, λ_{EX} = 480 nm) as reference standard, the quantum yield, Q_{QY}, of the QD-EG_{11}-Man and QD-EG_3-Man was determined as 6% and 4%, respectively. The Q_{QY} of this batch CdSe/ZnS QD prior to cap-exchange was 10%, thus cap-exchange led to considerable decrease of the QD Q_{QY}. This was not unexpected as similar results have been in literature.[4,5,15,16] Assuming a refractive index of 1.33

for the medium and random orientation of the dipoles (K^2 = 2/3), then the Förster radius (R_0, in the unit of Å) of the above QD-dye FRET pair (at 1:1 molar ratio) can be calculated by the equation[17]:

$R_0 = (8.79 \times 10^{-5} n_r^{-4} \times Q_{QY} \times K^2 \times I)^{1/6}$

For QD-EG$_3$-DiMan,

$R_0 = (8.79 \times 10^{-5} \times 1.33^{-4} \times 0.04 \times (2/3) \times 3.52 \times 10^{15})^{1/6}$ = 37 Å = 3.7 nm

For QD-EG$_{11}$-DiMan,

$R_0 = (8.79 \times 10^{-5} \times 1.33^{-4} \times 0.06 \times (2/3) \times 3.52 \times 10^{15})^{1/6}$ = 40 Å = 4.0 nm

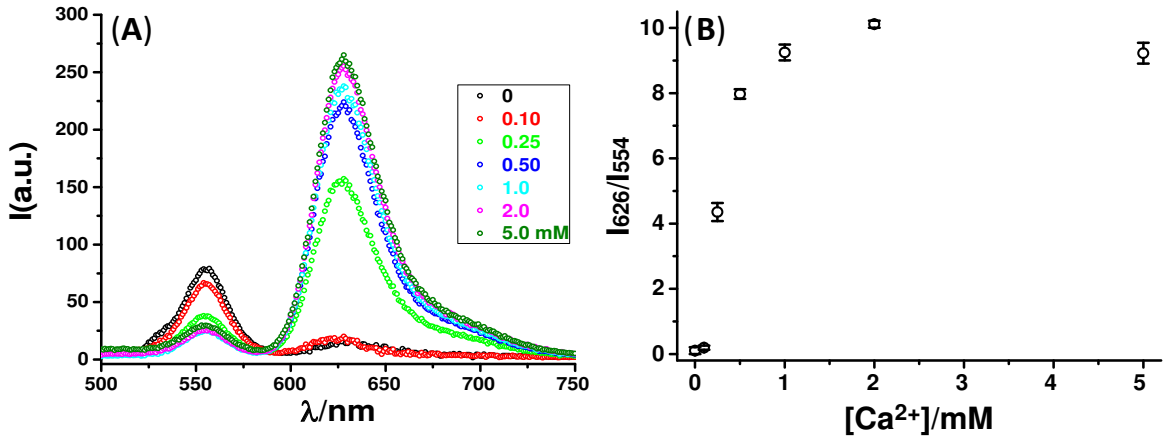

Figure S4: Ca^{2+}-dependent binding between DC-SIGN and QD-EG$_3$-DiMan. (**A**) Dye-direct excitation background corrected fluorescence spectra showing the binding of DC-SIGN (200 nM) with 20 nM of QD-EG$_3$-DiMan in the HEPES buffer (20 mM HEPES, 100 mM NaCl, pH=7.8) with different amounts of Ca^{2+}. (**B**) Relationship between the apparent FRET ratio (I_{626}/I_{554}) and Ca^{2+} concentration.

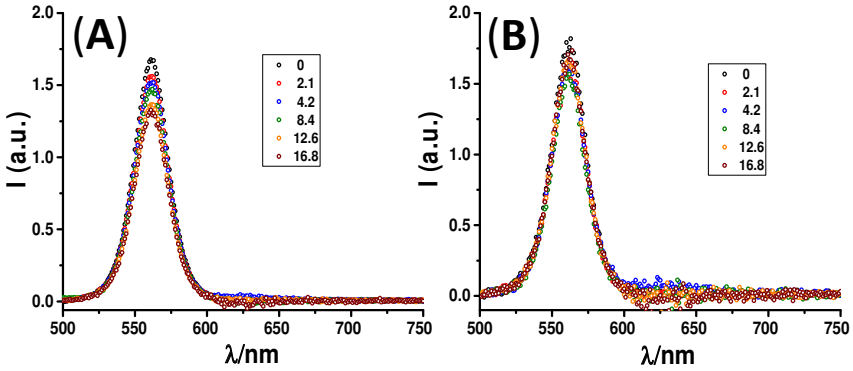

Figure S5: Dye-direct excitation background corrected fluorescent spectra of monovalent DC-SIGNR CRD after binding to QD-EG$_{11}$-DiMan (**A**) and QD-EG$_3$-DiMan (**B**) in binding buffer.

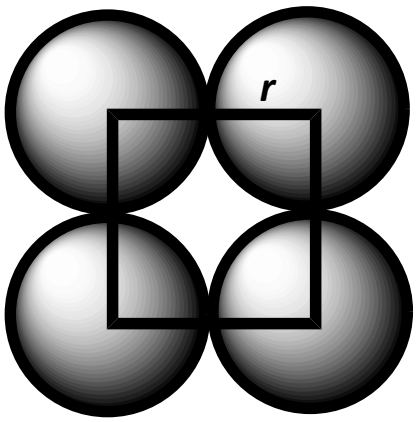

Figure S6: Schematic presentation of the cross-section of a DC-SIGN tetramer, where each CRD is assumed as a rigid ball of 3 nm diameter based on its crystal structure size.[18] The minimum cross-sectional foot print for each tetramer can be estimated as: $(2r)^2 + 4 \times (3/4)\pi r^2 = 3^2 + 3 \times 3.14 \times 1.5^2 = 30.2$ nm^2

Assuming the QD surface bound DC-SIGNs are closely packed with packing efficiency of 86%, then the surface area occupied by each DC-SIGN head = 30.1/0.86 = 35.1 nm^2

The natural surface area for QD-EG$_n$-DiMan can be estimated as $A = \pi D^2$, where D = D_h of the QD measured by dynamic light scattering.

For n = 3, $A = \pi D^2 = 3.14 \times 8.3^2 = 216$ nm^2

For n = 11, $A = \pi D^2 = 3.14 \times 9.5^2 = 283$ nm^2

The number of DC-SIGNs (N) that can pack on the QD surface without inducing crowding effect is estimated as:

N = 216/35.1 = 6.1 for QD-EG$_3$-DiMan

N = 283/35.1 = 8.1 for QD-EG$_{11}$-DiMan.

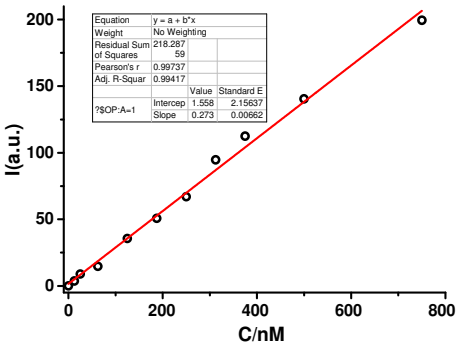

Figure S7: Relationship between the peak fluorescence intensity of Atto594 labeled DC-SIGN at 626 nm as a function of protein concentration: data were fitted by linear relationship: y = a + b*x, where a = 1.6 ±2.2; b = 0.273 ± 0.007, $R^2 = 0.994$. Note $C_{protein}$ = 800 nM corresponds to a PQR of 20 in the QD-FRET measurement where C_{QD} = 40 nM.

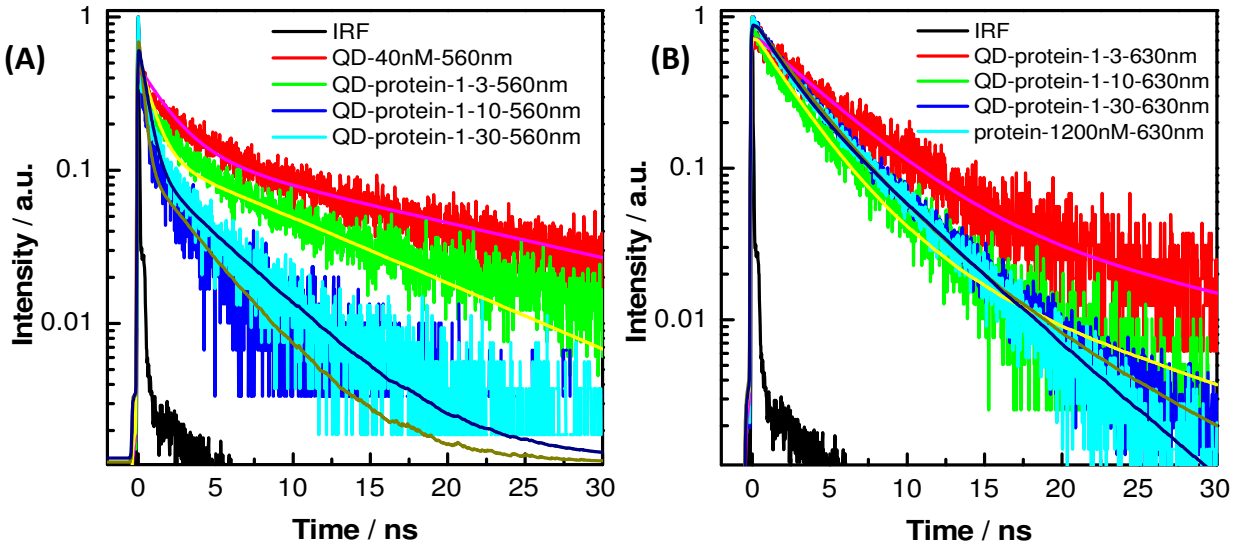

Figure S8: Typical decay curves for the QD fluorescence (**A**, λ_{EM} ~560 nm) and Atto594 FRET signal (**B**, λ_{EM} ~630 nm) for QD-EG_{11}-DiMan in binding buffer before (red) and after binding to Atto594 labeled DC-SIGN under different protein:QD molar ratios (PQRs): 3 (green), 10 (blue) and 30 (cyan). The instrument response (IRF) was shown in black.

The QD-EG_{11}-DiMan fluorescence lifetime after mixing with different molar ratio of Atto594 labeled DC-SIGN: the QD decay curves (**Figure S8A**) were fitted by bi-exponential decay with fitting parameters listed below. The lifetime is calculated by: $\tau = \tau_1 \times \alpha_1 + \tau_2 \times \alpha_1$

Sample	**α_1**	**τ_1 (ns)**	**α_2**	**τ_2 (ns)**	**τ (ns)**
QD only	0.26	1.87	0.74	19.28	14.75
QD + DC-SIGN (1:3)	0.25	0.72	0.75	10.10	7.76
QD + DC-SIGN (1:10)	0.44	0.26	0.56	2.93	1.76
QD + DC-SIGN (1:30)	0.48	0.50	0.52	4.04	2.34

The fluorescence lifetime of the Atto594 the decay curves (**Figure S8B**) were fitted by bi-exponential decay with fitting parameters listed below. The lifetime is calculated by $\tau = \tau_1 \times \alpha_1 + \tau_2 \times \alpha_1$

Sample	**α_1**	**τ_1 (ns)**	**α_2**	**τ_2 (ns)**	**τ (ns)**
QD + DC-SIGN (1:3)	0.75	3.91	0.25	20.89	8.16
QD + DC-SIGN (1:10)	0.84	2.46	0.16	12.09	4.00
QD + DC-SIGN (1:30)	0.82	2.65	0.18	7.04	3.44
DC-SIGN only	0.39	1.92	0.61	4.48	3.48

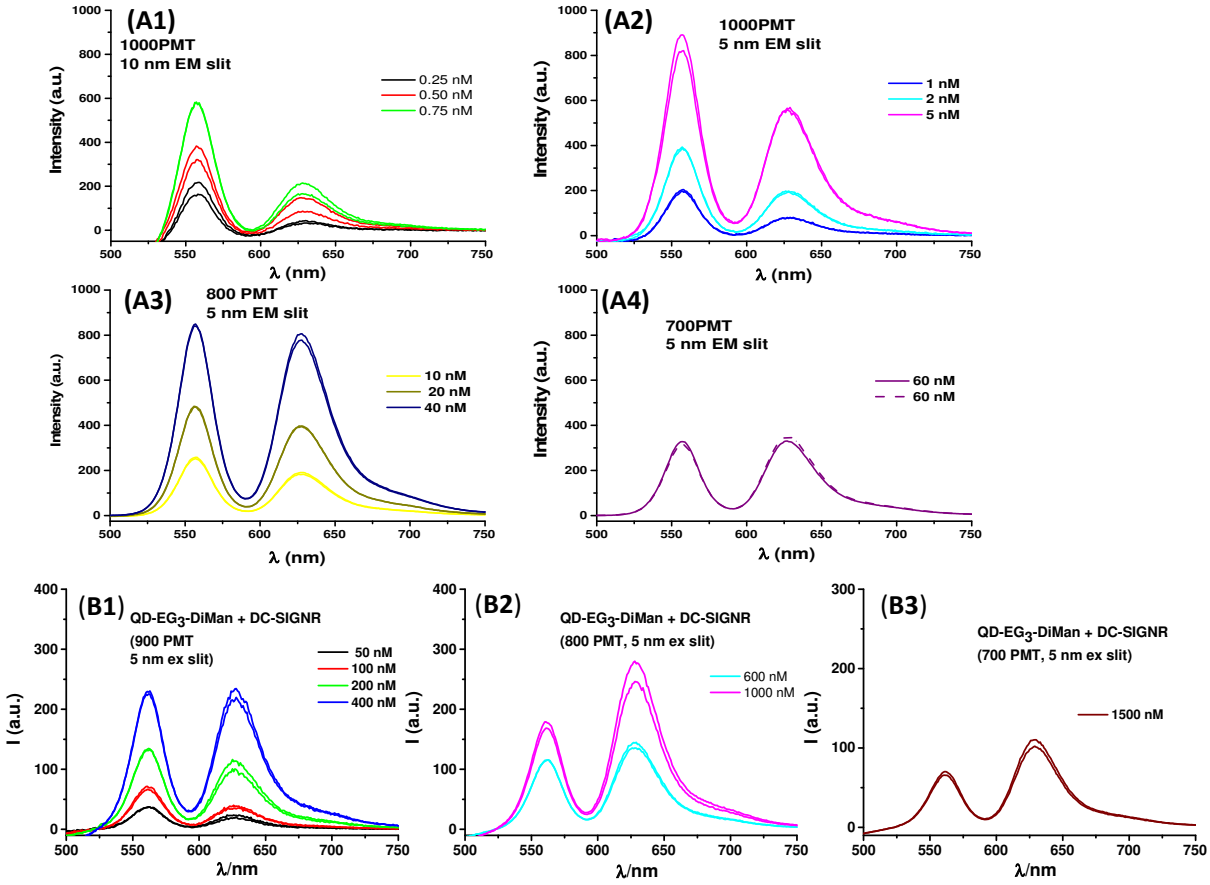

Figure S9: Representative fluorescence spectra (each concentration done in duplicate given in each colour) used to determine the K_ds of the QD-DiMan-DC-SIGN/R bindings. All spectra were corrected by the direct excitation background recorded with the same concentration labeled protein only under identical conditions.

(**A1-A4**) Fluorescence spectra of QD-EG_3-Man:DC-SIGN (1:1 molar ratio) mixture at different concentrations in binding buffer containing 1 mg/mL of BSA. Different spectral recording conditions (PMT voltage and emission slit width) were used to compensate for the very different QD/protein concentrations (fluorescence intensity). Although the different conditions may affect the absolute fluorescence intensity, the resulting apparent FRET ratio (a ratiometric signal) is not affected.

(**B1-B3**) Fluorescence spectra of the 1:10 (molar ratio) QD-EG_3-Man and DC-SIGNR mixture at different concentrations in binding buffer containing 1 mg/ml of BSA. Different spectral recording conditions (PMT voltage and emission slit width) were used to compensate for the different QD/protein concentrations (absolute fluorescence intensity).

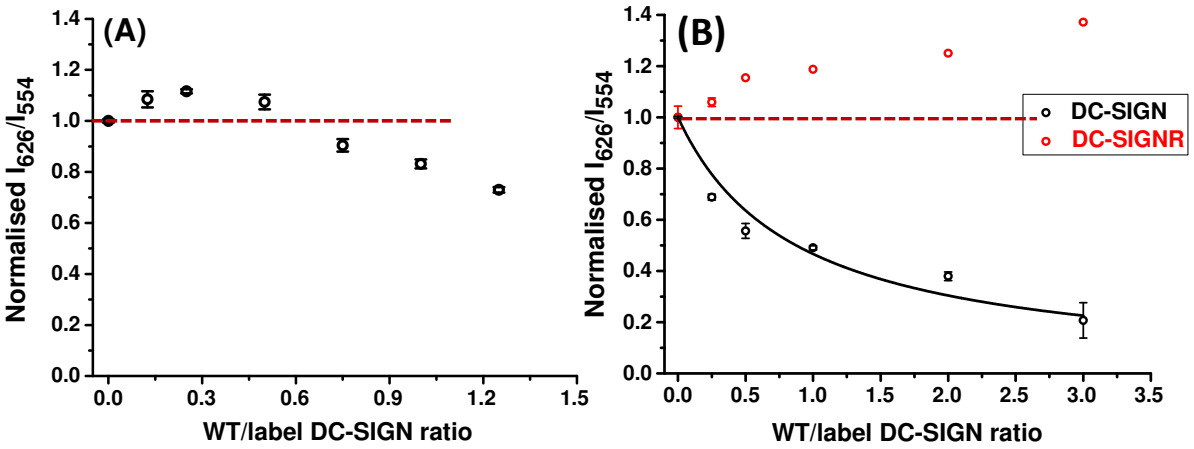

Figure S10: (**A**) Relationship between the normalised I_{626}/I_{554} ratio and the unlabeled wild-type DC-SIGN:labeled DC-SIGN molar ratio for binding to QD-EG_{11}-DiMan (100% glycan density). (**B**) Relationship between the normalised I_{626}/I_{554} ratio and unlabeled wild-type DC-SIGN or DC-SIGNR:labeled DC-SIGN molar ratio on binding to QD-EG_{11}-DiMan (25% glycan density, with the rest ligand being DHLA-zwitterion). Data were fitted by the competition modal. The broken red line (for guiding the eye) indicates no change of the apparent FRET ratio.

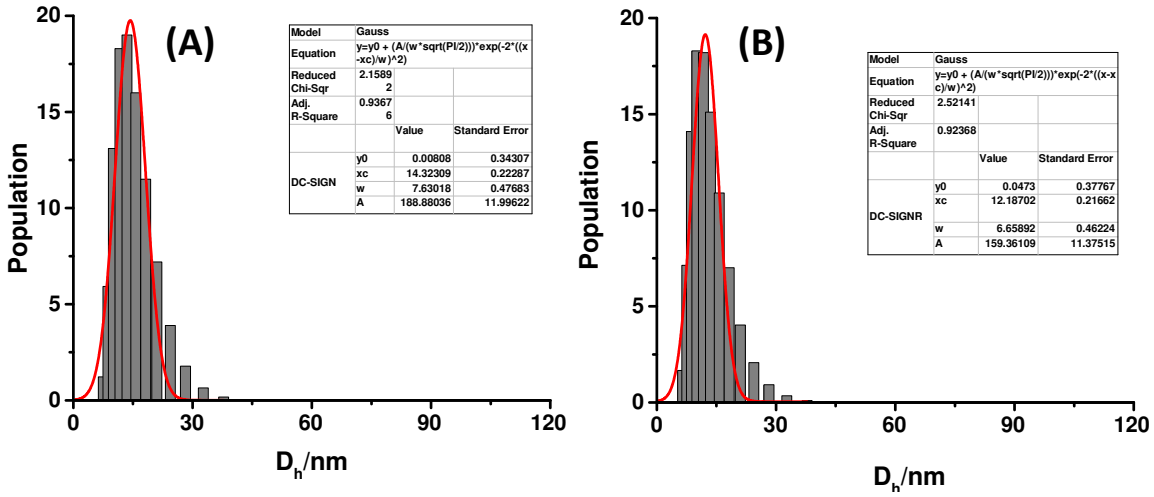

Figure S11: Hydrodynamic diameter (D_h, volume population) histograms of DC-SIGN (**A**) and DC-SIGNR (**B**) in binding buffer measured by dynamic light scattering. The histograms were fitted by standard Gaussian function, giving a D_h value of 14.3±0.2 and 12.2±0.2 nm for DC-SIGN and DC-SIGNR, respectively.

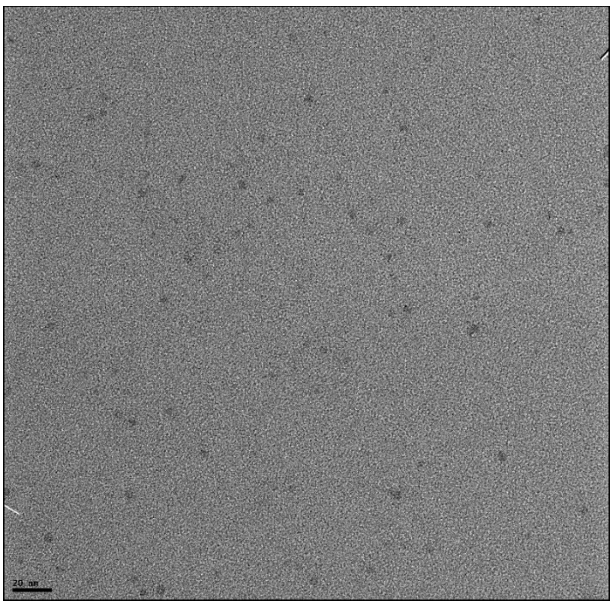

Figure S12. A typical bright field TEM image of QD-EG_{11}-DiMan dispersed in pure water. All QDs appear as isolated particles without aggregation. Scan bar = 20 nm.

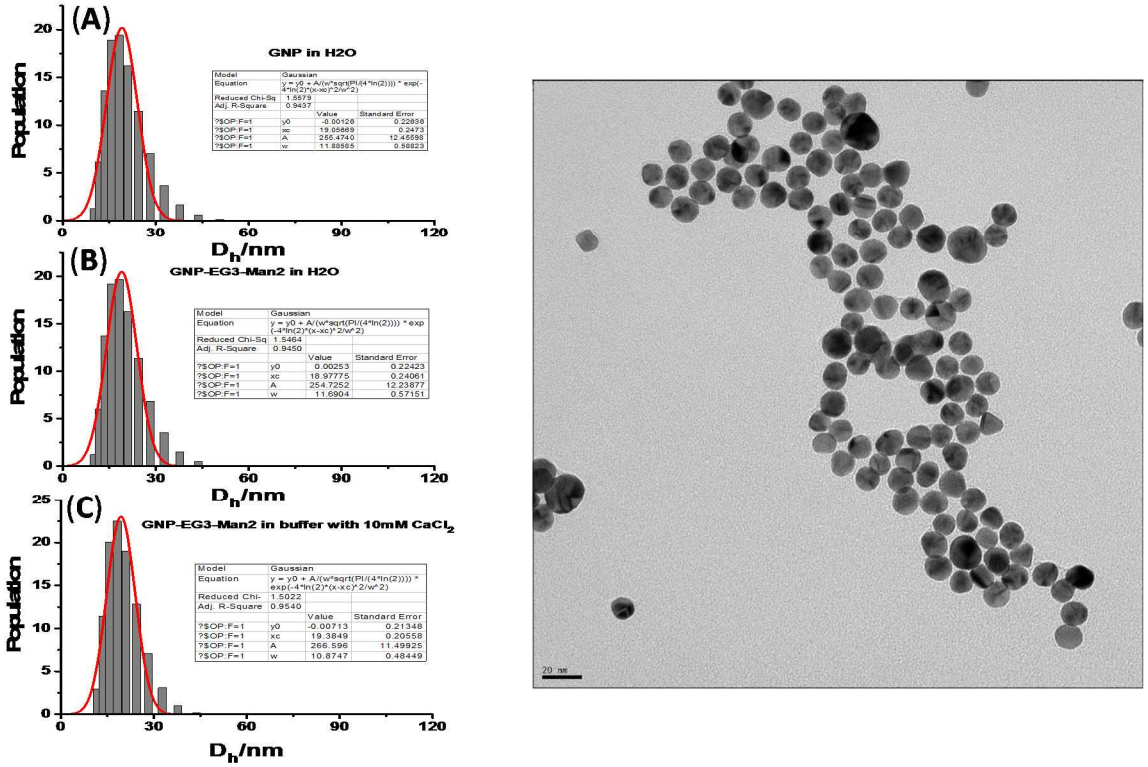

Figure S13: Left: Hydrodynamic diameter (D_h) volume distribution histograms of the synthesised GNP in pure H_2O (**A**) and GNP-GE_3-DiMan in H_2O (**B**) and in binding buffer containing 10 mM $CaCl_2$ (**C**) measured by dynamic light scattering. A mean D_h of ~19 nm was obtained for the GNP. **Right**: typical TEM bright field image of the GNP in water, scale bar = 20 nm.

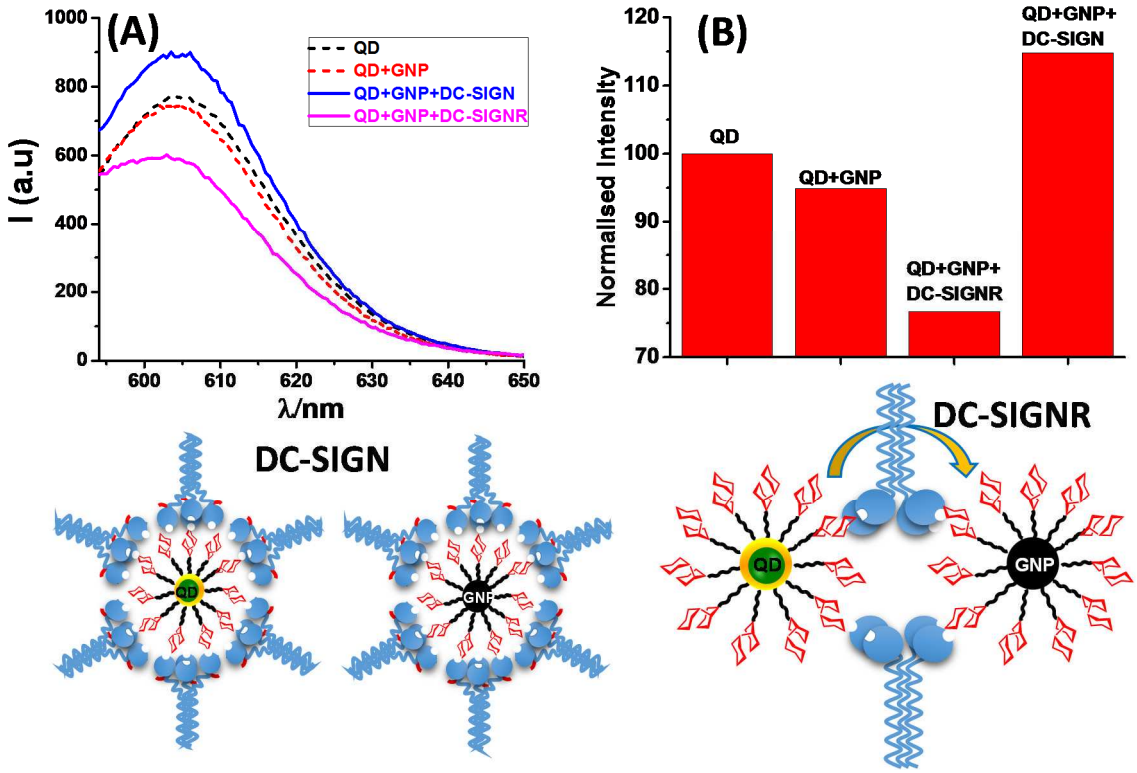

Figure S14. (**A**) Fluorescence spectra of the CdSe/ZnSe/ZnS QD-EG_3-DiMan (λ_{EM} ~605 nm, 10 nM) only (black) or QD-EG_3-DiMan (10 nM) + GNP-EG_3-DiMan (5 nM) mixtures in the absence (red) and presence of 125 nM of wild-type DC-SIGN (blue) or DC-SIGNR (pink). (**B**) Comparison of the integrated QD fluorescence intensities of the above samples. All data were normalised by the QD-EG_3-DiMan only (QD, set as 100). The schematics below show the DC-SIGN/R binding behaviours accounting for the different QD fluorescence: binding of multiple DC-SIGNs to the QD or GNP not only prevent their assembly, but also break up any pre-assembled QDs in clusters in binding buffers, leading to QD fluorescence increases; whereas DC-SIGNR cross-links the QD and GNP, leading to significant QD fluorescence quenching by the proximity GNP.

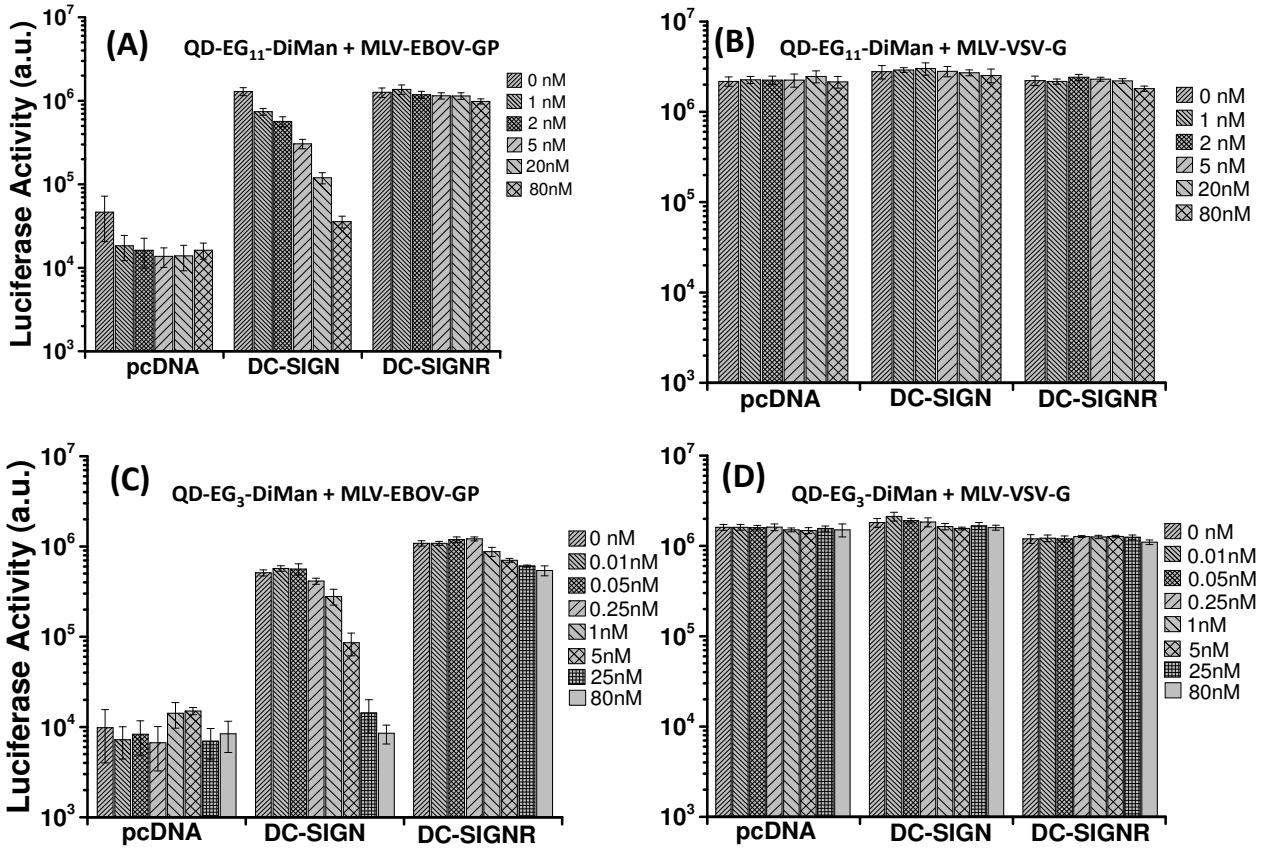

Figure S15: Comparison of cellular luciferase activities of 293T cells after being transfected with the indicated plasmids, pre-incubation with QD-EG_{11}-DiMan (**A, B**) or QD-EG_3-DiMan (**C, D**) and followed by inoculation with MLV reporter particles bearing the EBOV-GP (**A, C**) or the control VSV-G (**B, D**). The indicated QD concentrations were attained after addition of particles. Luciferase activities in cell lysates were measured at 72 h post-transduction. The results of single experiments performed with quadruplicate samples are shown. Error bars indicate the standard deviation. The inhibition results were confirmed in three separate experiments.

11: References

(1) Guo, Y.; Sakonsinsiri, C.; Nehlmeier, I.; Fascione, M. A.; Zhang, H.; Wang, W.; Poehlmann, S.; Turnbull, W. B.; Zhou, D. *Angew. Chem. Int. Ed.* **2016**, *55*, 4738.

(2) Zhang, H.; Feng, G.; Guo, Y.; Zhou, D. *Nanoscale* **2013**, *5*, 10307.

(3) Zhang, H.; Li, S.; Lu, R.; Yu, A. *Acs Appl. Mater. Interfaces* **2015**, *7*, 21868.

(4) Susumu, K.; Uyeda, H. T.; Medintz, I. L.; Pons, T.; Delehanty, J. B.; Mattoussi, H. *J. Am. Chem. Soc.* **2007**, *129*, 13987.

(5) Mei, B. C.; Susumu, K.; Medintz, I. L.; Mattoussi, H. *Nat. Protoc.* **2009**, *4*, 412.

(6) Zhan, N. Q.; Palui, G.; Grise, H.; Tang, H. L.; Alabugin, I.; Mattoussi, H. *ACS Appl. Mater. Interfaces* **2013**, *5*, 2861.

(7) Zhou, D.; Ying, L.; Hong, X.; Hall, E. A.; Abell, C.; Klenerman, D. *Langmuir* **2008**, *24*, 1659.

(8) Zhang, H.; Zhou, D. *Chem. Commun.* **2012**, *48*, 5097.

(9) Guo, Y.; Feinberg, H.; Conroy, E.; Mitchell, D. A.; Alvarez, R.; Blixt, O.; Taylor, M. E.; Weis, W. I.; Drickamer, K. *Nat. Struct. Mol. Biol.* **2004**, *11*, 591.

(10) Feinberg, H.; Guo, Y.; Mitchell, D. A.; Drickamer, K.; Weis, W. I. *J. Biol. Chem.* **2005**, *280*, 1327.

(11) Hill, H. D.; Millstone, J. E.; Banholzer, M. J.; Mirkin, C. A. *Acs Nano* **2009**, *3*, 418.

(12) Hondow, N.; Brydson, R.; Wang, P.; Holton, M. D.; Brown, M. R.; Rees, P.; Summers, H. D.; Brown, A. *J. Nanopart. Res.* **2012**, *14*.

(13) Kong, Y. F.; Chen, J.; Fang, H. W.; Heath, G.; Wo, Y.; Wang, W. L.; Li, Y. X.; Guo, Y.; Evans, S. D.; Chen, S. Y.; Zhou, D. J. *Chem. Mater.* **2016**, *28*, 3041.

(14) Song, L.; Ho, V. H. B.; Chen, C.; Yang, Z. Q.; Liu, D. S.; Chen, R. J.; Zhou, D. J. *Adv. Healthcare Mater.* **2013**, *2*, 275.

(15) Zhang, Y.; Zhang, H.; Hollins, J.; Webb, M. E.; Zhou, D. *Phys. Chem. Chem. Phys.* **2011**, *13*, 19427.

(16) Zhou, D. J.; Li, Y.; Hall, E. A. H.; Abell, C.; Klenerman, D. *Nanoscale* **2011**, *3*, 201.

(17) Charbonniere, L. J.; Hildebrandt, N. *Eur. J. Inorg. Chem.* **2008**, 3241.

(18) Feinberg, H.; Mitchell, D. A.; Drickamer, K.; Weis, W. I. *Science* **2001**, *294*, 2163.